Available online at www.sciencedirect.com
ScienceDirect
Journal of Volcanology and Geothermal Research 168 (2007) 68–92
Journal of volcanology and geothermal research
www.elsevier.com/locate/jvolgeores

High water contents in basaltic magmas from Irazú Volcano, Costa Rica

Ezra R. Benjamin [a,1], Terry Plank [a,*], Jennifer A. Wade [a,2], Katherine A. Kelley [b,3], Erik H. Hauri [b], Guillermo E. Alvarado [c]

[a] *Department of Earth Sciences, Boston University, Boston, MA 02215, USA*
[b] *Department of Terrestrial Magnetism, Carnegie Institution of Washington, Washington, DC 20015, USA*
[c] *Universidad de Costa Rica and Instituto Costarricense de Electricidad, San José, Costa Rica*

Received 13 January 2007; accepted 8 August 2007
Available online 28 August 2007

Abstract

Irazú volcano, in Costa Rica, erupts magmas unusually enriched in incompatible trace elements (e.g., K, REE) relative to most other arc volcanoes worldwide. Previous studies place this enrichment in the mantle, with minimal inputs from the subducting slab. In order to test the subduction vs. mantle hypotheses, we present here the first published measurements of the pre-eruptive volatile content of Irazú magmas. Olivine-hosted melt inclusions from basaltic–andesite scoria from the 1723 eruption are volatile-rich, containing >3 wt.% H_2O, >200 ppm CO_2, >2500 ppm S, >2200 ppm Cl and >1800 ppm F. The average composition of the 1723 melt inclusions is very similar to that of the host scoria (SiO_2=54% SiO_2), although inclusions include more mafic (48% SiO_2) and felsic (57% SiO_2) compositions. The 1723 melt inclusions have the same trace element characteristics (e.g., Ba/La) as the host scoria, ruling out exotic crustal or mantle sources. Together, the melt inclusions and their host olivines ($Fo_{87–79}$) define a closed-system ascent path (150–20 MPa) of coupled degassing, crystallization, and cooling (1075–1045 °C). The maximum H_2O measured in the melt inclusions and the shape of the degassing path together constrain the pre-eruptive H_2O content to 3.2–3.5 wt. %, significantly higher than in ocean island basalts, but typical of arc magmas. The high H_2O in Irazú melts, coupled with their high Cl/K_2O, are inconsistent with enriched mantle with minimal slab fluid addition. We propose instead that subducting input is the dominant contributor to Irazú's geochemical compositions. Galapagos-derived seamounts and volcaniclastics are currently entering the trench near Irazú, and provide to the Irazú source both volatiles (from seafloor hydration and chlorination) and ocean–island-type trace elements and isotopes. A few percent of subducted Galapagos volcanics added to MORB mantle can create Irazú compositions quantitatively, provided elements are further fractionated according to solute-rich liquid or melt–eclogite partition coefficients. Subduction of seamount chains may create high-K arc volcanism elsewhere, such as in the northern Marianas.

Keywords: volatiles; arc; subduction; geochemistry; mantle

* Corresponding author. Tel.: +1 617 353 4213; fax: +1 617 353 3290.
E-mail address: tplank@bu.edu (T. Plank).
[1] Now at: Environmental Resources Management, Boston, MA 02116 USA.
[2] Now at: Library of Congress, Preservation Research and Testing, Washington, DC 20540, USA.
[3] Now at: University of Rhode Island, Graduate School of Oceanography, Narragansett, RI 02882 USA.

0377-0273/$ - see front matter © 2007 Elsevier B.V. All rights reserved.
doi:10.1016/j.jvolgeores.2007.08.008

1. Introduction

Irazú Volcano is an active arc volcano at the southeastern terminus of the Central American Volcanic arc (CAVA) in Costa Rica (Fig. 1). The geochemical composition of volcanic rocks from Irazú and neighboring volcanoes are unusual both within the CAVA and within the spectrum of global arc compositions. For example, the CAVA records systematic along-strike variations in many geochemical tracers of the slab (Fig. 2), including Ba/La (Carr et al., 1990), $^{238}U/^{230}Th$ (Herrstrom et al., 1995), U/Th (Patino et al., 2000), $^{10}Be/^{9}Be$ (Morris et al., 1990), B/Be (Leeman et al., 1994), and $\delta^{18}O$ (Eiler et al., 2005). For most of these tracers, the peak in inferred slab flux occurs in the central portion of the CAVA, in Nicaragua, and falls to nearly the global minimum to the southeast, at the terminal sector of volcanoes that includes Irazú. At the same time, the concentrations of many trace elements are highly enriched in Irazú magmas relative to the CAVA or arcs worldwide. Irazú magmas possess among the highest La/Sm of any arc volcano (Fig. 3a), and their REE patterns (Fig. 3b) resemble those of ocean island basalts (OIB).

Taken together, the OIB-type ratios but high concentrations of trace elements have led many workers to propose that Irazú magmas are generated from enriched mantle, like OIB, with little input from the subducting plate. Carr et al. (1990) suggested that enriched mantle preferentially melts beneath Costa Rica due to a spatially diffuse slab fluid flux caused by a shallow slab dip. Leeman et al. (1994) proposed that Costa Rica magmas tap enriched components in the mantle lithosphere. Herrstrom et al. (1995) suggested that trench-parallel flow around the end of the Cocos slab has driven enriched mantle beneath Irazú, citing evidence from seismic anisotropy measurements (Russo and Silver, 1994). Clark et al. (1998) called upon mantle-derived carbonatites in the source of Irazú magmas, while Feigenson et al. (2004) proposed mantle enrichment caused by the Cretaceous passage of the Galapagos hotspot. The implication from many of these studies is that enriched mantle dominates the abundance of most trace elements relative to the slab flux (Reagan and Gill,

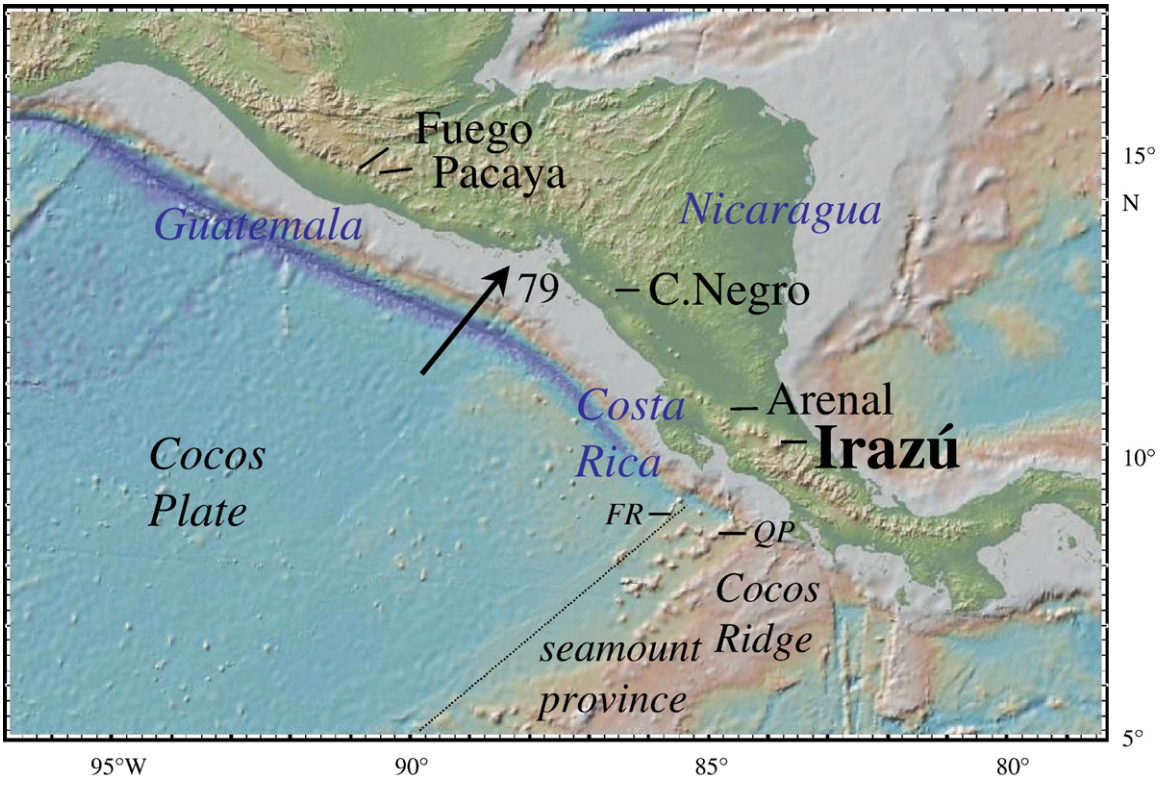

Fig. 1. Location of Irazú volcano within the Central American volcanic arc. Other active volcanoes shown for which H_2O contents have been determined in melt inclusions. Cocos Ridge and seamount province derive from the Galapagos hot spot (Hoernle et al., 2000). FR (Fisher Ridge) and QP (Quepos Plateau). Basemap from GeoMapApp. Plate motion vector, with velocity in mm/yr, calculated from Cocos–Caribbean pole in DeMets (2001).

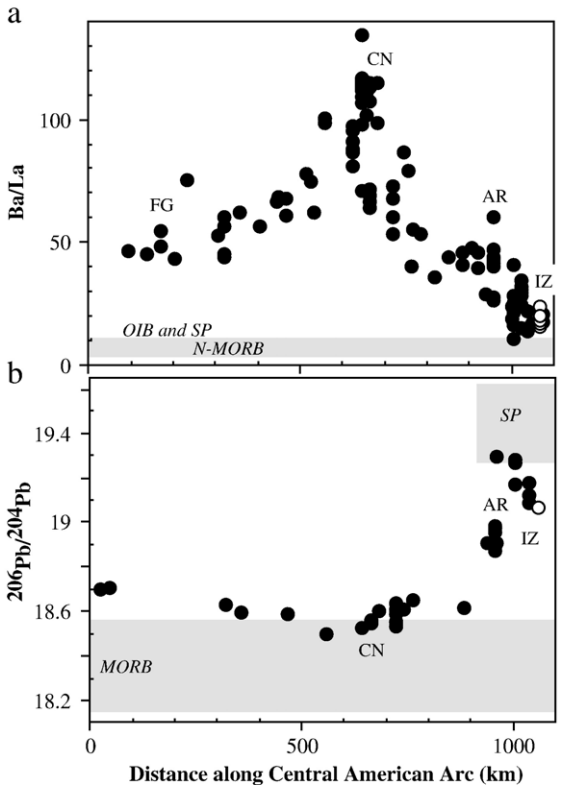

Fig. 2. Geochemical variations along-strike of the Central American arc (measured as distance from the Guatemala–Mexico border). a) Ba/La in basalts (<53% SiO_2 or >3% MgO), as in Plank et al. (2002) and from Carr et al. (2003). b) Pb isotope ratios from Feigenson et al. (2004). Irazú (IZ), Arenal (AR), Cerro Negro (CN) and Fuego (FG) volcanoes identified. Ba/La for normal-mid ocean ridge basalts (N-MORB) and ocean island basalts (OIB) from Sun and McDonough (1989). MORB Pb isotope average +/− one standard deviation for East Pacific Rise basalts from PetDB (2007). SP is average of seamount province on Cocos Plate, seaward of Arenal to Irazú, derived from the northern domain of the Galapagos hot spot (Hoernle et al., 2000).

1989; Carr et al., 1990; Patino et al., 2000), but other studies also emphasize a lesser slab flux beneath Costa Rica as compared to Nicaragua, due to a greater degree of hydration of the Nicaragua slab (Rupke et al., 2002; Abers et al., 2003; Eiler et al., 2005;), a hotter Costa Rica slab (Leeman et al., 1994), or loss of material from the slab during subduction beneath Costa Rica (Morris et al., 2002).

Recent studies of igneous forearc complexes of Costa Rica and of the incoming Cocos plate seaward of Costa Rica lead to alternative models for the unusual geochemical composition of magmas in the southern end of the Costa Rica arc. Both regions include material derived from the Galapagos hot spot. The Costa Rica forearc is composed of Cretaceous to Tertiary igneous complexes with a Galapagos affinity (Hauff et al., 2000; Hoernle et al., 2002). The incoming Cocos plate includes 14 Ma seamounts and plateaux that are geochemically zoned in geographical domains that mimic those of the modern Galapagos hot spot (Werner et al., 1999; Hoernle et al., 2000). The erosion of this forearc material on the one hand (von Huene et al., 2000; Vannucchi et al., 2003; Goss and Kay, 2006), and the subduction of it on the other (Hoernle et al., 2006), would lead to exotic input to this part of the CAVA, and create an arc dominated by Galapagos OIB input. Galapagos input in general, and the seamount province in particular, explain well the dramatic increase in

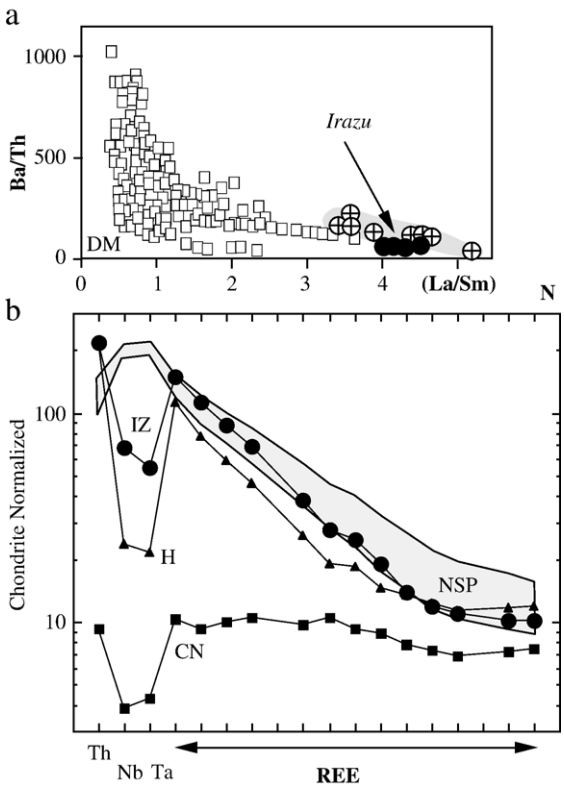

Fig. 3. a) Irazú volcanics (solid circles) in the context of global island arc compositions (from Elliott, 2003; La/Sm normalized to primitive mantle in Sun and McDonough, 1989). Irazú volcanics are among the highest globally in La/Sm; along with the northern Mariana seamount province, ~23–25°N (circle with plus, shaded field). Irazú data from Table 1. b) Chondrite normalized REE diagram, including Th, Nb, and Ta. 1723 Irazú tephra (Table 1) compared to Cerro Negro lava, Nicaragua (CN-92-2 from Thomas et al., 2002), and Hiyoshi island in the northern Marianas seamount province (Peate and Pearce, 1998). Shaded field is average and one standard deviation of samples from the northern seamount province (NSP) of Hoernle et al. (2000). Note negative Nb–Ta anomalies in arc samples (IZ, CN, H), positive ones in the Galapagos-related NSP samples, and similarity between Irazú and Hiyoshi patterns.

$^{206}Pb/^{204}Pb$ in the southern sector of the CAVA arc, which includes Irazú volcano (Fig. 2b). These hypotheses differ from previous ones in that the OIB signature in Irazú magmas derives from the subduction zone, instead of the sub-arc mantle.

One possible test of hypotheses as to the source of Irazú magmas is their water content. Water is perhaps the most obvious tracer of subducted material, and is notably high in concentration in arc magmas (generally >2 wt.%; Wallace, 2005) and much lower in MORB (<0.5) and back-arc basalts (<2 wt.% H_2O; Kelley et al., 2006). No published data exist for H_2O in Galapagos island magmas, but Galapagos-influenced magmas along the Galapagos Spreading Center have <1.5 wt.% H_2O (Cushman et al., 2004), like ocean island basalts elsewhere (Dixon et al., 1997, 2002; Workman et al., 2006). If Irazú taps an enriched mantle, with a weak subduction component, then it might be expected to erupt magmas with a lower water content than is typical of arc basalts. For example, enriched mantle with <0.04 wt.% H_2O (Dixon et al., 2002) would generate low water contents of <0.65 wt.% in Irazú primary melts, assuming 5.5% mantle melting (Eiler et al., 2005) and a mantle/melt partition coefficient for H_2O of 0.007 (Hauri et al., 2006). Mantle with high $^3He/^4He$ (i.e., >8 times the atmospheric ratio, R_A) might have higher H_2O contents of 0.075 wt.% (e.g., FOZO in Dixon et al., 2002), but fumaroles related to Irazú vent gases that are unremarkable, and within the MORB range for $^3He/^4He$ (i.e., 8+/−1 R_A; Shaw et al., 2003). Adding a small subduction component has little effect on this calculation. For example, Eiler et al. (2005) calculate an Irazú source with 0.35% of a slab fluid/melt that contains 10 wt.% H_2O. If added to the enriched mantle above (<0.04 wt.% H_2O), this fluid/melt would raise the source to 0.075 wt.% H_2O, and the magmas to 1.2 wt.% H_2O, still atypical of arc basalts. Thus, if Irazú sources are dominated by enriched mantle with a low slab flux, then low water contents would be expected in these magmas ($\leq \sim 1$ wt.% H_2O). On the other hand, if Irazú sources are dominated by input of altered and hydrated OIB material from the forearc and/or incoming plate, then higher H_2O contents might be expected (>1 wt.% H_2O), more typical of arc magmas elsewhere (Wallace, 2005). With these predictions in mind, we report here the volatile content of melt inclusions from the recent eruptions of Irazú Volcano.

1.1. Irazú, Volcano, Costa Rica

Irazú volcano is located 24 km east of San Jose, on the continental divide of Costa Rica, and rises to 3432 m in elevation. Irazú is one of the largest volcanoes in the CAVA, with a volume of roughly 227 km^3 (Carr et al., 2003). It is the pinnacle of the group of volcanoes that comprises the Central Cordillera, which marks the terminus of the CAVA. The cessation of volcanism to the southeast of Irazú coincides with subduction of the Cocos Ridge, a volcanic constructional feature <14 Ma, which can be traced bathymetrically and geochemically to the active Galapagos hot spot (Kolarsky et al., 1995; Werner et al., 1999; Hoernle et al., 2000; Fig. 1). Other seamounts, plateaux and volcaniclastics of similar composition and age lie on the seafloor northwest of the Cocos Ridge, and are currently subducting at the trench offshore of Irazú volcano (Hoernle et al., 2000; Fig. 1). Carr et al. (2003) and von Huene et al. (2000) propose that the line of volcanoes from Platanar to Irazú, which share distinctive geochemical characteristics (Fig. 2), form a segment related to subduction of the Fisher Ridge and Quepos Plateau on the downgoing plate (Fig. 1). The Fisher ridge is composed of mid-ocean-ridge-type basalts (Werner et al., 1999), while seamounts and plateaux to the southeast of Fisher (including the Quepos plateau) are composed of Galapagos-type volcanics that correlate isotopically to the northern domain of the Galapagos archipelago (Hoernle et al., 2000). Cretaceous and early Tertiary "ophiolites" linked to an earlier phase of Galapagos volcanism comprise the fore-arc of Irazú, and may also contribute material to the subduction zone via subduction erosion (Goss and Kay, 2006).

The major recent eruptions of Irazú Volcano in 1723 and 1963–1965 are the focus of this study. These strombolian and vulcanian eruptions were not only impressive markers in the history of Irazú, but also affected the lives of people who resided on and near the volcano (Murata et al 1966; Waldron, 1967; Alvarado, 1993). Although both eruptions are classified with a Volcanic Explosivity Index of 3, the 1723 eruption is considered the stronger of the two, based on the work of Alvarado (1993), who integrated study of the volcanic deposits with the detailed historic accounts of the Spanish governor Diego de la Haya. The eruption opened with a crater explosion and ash column, which yielded an initial open crater, and <10 cm of fine breccia and phreatic pyroclastic surge deposits. Violent strombolian activity ensued over the next few days, generating a new cinder cone, and depositing in the proximal facies a maximum of 6 m of scoria lapilli and bombs now exposed in the southern part of the Crater Principal (Alvarado, 1993). Events over the following months involved phreatomagmatic explosions, volcano–tectonic earthquakes, deposition of several ash layers from phreatomagmatic surges, and small lahars. The total

Table 1
Composition of Irazu scoria samples

Sample	IZ03-17a	IZ03-19b1 [b]	IZ03-19b2	91-71-16 [d]
	lapilli	*bomb*	*bomb*	*lapilli*
Age	1723	1963–5	1963–5	1963–5
UTM (E) [a]	552.7	552.6	552.6	
UTM (N)	218.2	218.1	218.1	
SiO_2	54.23	57.09	55.32	54.09
TiO_2	1.20	0.99	1.14	1.15
Al_2O_3	17.34	16.83	16.24	17.72
Fe_2O_3	8.15	7.48	7.84	8.09
MnO	0.138	0.124	0.129	0.135
MgO	4.66	5.55	4.95	4.75
CaO	8.94	8.06	7.75	8.83
Na_2O	3.50	3.41	3.51	3.40
K_2O	2.02	1.97	2.19	2.20
P_2O_5	0.49	0.39	0.45	0.45
Total	100.67	101.89	99.52	100.82
H_2O-	0.29	0.03	3.67	
LOI	−0.15	0.00	0.23	
Mg# [c]	58.6	64.8	61.0	
Vesicles	67.7	1.0		
G'mass	27.4	69.9		
Plag	3.3	22.9		
Cpx	1	3.8		
Ol	0.3	1.4		
Opx	0	0.6		
Oxides	0	0.4		
Total	99.7	100.0		
Li	9.36	10.7	10.7	9.6
Be	1.82	1.72	1.91	1.66
Sc	22.4	20.8	21.8	23.2
TiO_2	1.15	0.93	1.11	
V	217	184	202	224
Cr	69	136	113	77
Co	26.5	26.3	25.1	25.9
Ni	39.8	80.2	49.6	39.8
Cu	121	124	126	116
Zn	79.2	75.4	80.3	77.2
Rb	54.7	57.6	62.1	58.7
Sr	820	814	754	820
Y	26.2	20.0	23.9	26.6
Zr	229	202	242	231
Nb	23.0	20.6	24.8	23.3
Cs	0.725	0.902	0.917	0.730
Ba	857	824	859	875
La	49.2	41.3	47.1	48.8
Ce	96.2	79.6	92.2	99.9
Pr	11.4	9.3	10.8	12.0
Nd	44.0	35.0	40.8	44.6
Sm	7.73	6.05	7.10	7.87
Eu	2.14	1.65	1.87	2.11
Gd	6.84	5.28	6.19	6.47
Tb	0.97	0.75	0.89	1.02
Dy	4.79	3.66	4.38	5.01
Ho	0.91	0.70	0.83	0.92
Er	2.49	1.91	2.28	2.49
Yb	2.23	1.75	2.06	2.25
Lu	0.347	0.272	0.319	0.348
Hf	4.68	4.28	5.05	5.26
Ta	1.16	1.11	1.32	1.22
Pb	5.55	5.79	6.24	5.73
Th	8.77	9.80	10.59	9.78
U	3.09	3.51	3.76	3.44

Major elements (wt.%) by ICP-ES following ignition and fusion with $LiBO_2$. Modal analyses based on 300–500 points. Trace elements (ppm) by ICP-MS following digestion with HF:HNO3 in screw-top teflon vials. Major and trace elements calibrated using standard values for BIR, K1919 and BHVO from Kelley et al. (2003).

[a] UTM locations: Istaru Quad. Basemap.

[b] 19b1 and 19b2 are two separate bombs from sample IZ03-19b.

[c] Mg# calculated assuming 20% total Fe as Fe3+ (as in Table 2).

[d] Analysis reproduced from Clark et al. (1998) for convenience.

duration of the eruption was at least 10 months (Alvarado, 1993).

The 1963–1965 eruption lasted 30 months, involving vulcanian (phreatomagmatic) and strombolian phases that constituted four stages (the following summary is from Alvarado, 1993; Alvarado et al., 2006). Stage 1 (Feb to Dec 9, 1963) was marked by occasional strong explosive phases, with maximum observed ash column heights up to 11 km, and bombs that fell up to 7 km from the crater. Stage 2 (Dec 19, 1963 to Jan 1964) was the period of greatest activity, with the frequent eruption of scoria and bread-crust bombs. Stage 3 (Feb to Aug, 1964) was marked by declining production of ash and bombs, and Stage 4 (Sept, 1964 to Feb, 1965), was the final, waning stage. Stages 1 and 2 intracrater deposits are dominated by ballistic strombolian beds, while Stages 3 and 4 are dominated by pyroclastic flow deposits. The deposits of the eruption reached a maximum thickness of 25.5 m near the crater rim, with a total volume of tephra estimated at 0.2–0.3 km^3 (dense rock equivalent). Heavy ash falls were reported in downtown San Jose, which at times were so intense that they blocked the midday sun (Murata et al., 1966; Alvarado and Schmincke, 1994). Landslides and lahars were most pronounced along the Reventado River (Murata et al., 1966), and the cost of damage to the surrounding area has been estimated at 100–200 million dollars (Alvarado, 1993). Thus, both eruptions produced exclusively pyroclastic deposits, although a small lava pool was present in both eruptions. Lava flows were generated by previous volcanic activity at Irazú (Alvarado, 1993; Alvarado et al., 2006).

Although Irazú has erupted a range of compositions, from primitive basalt (Mg#∼67) to dacite (SiO_2 ∼63 wt.% SiO_2), the 1723 and 1963–5 eruptions consist largely of high potassium (∼2 wt.%) basaltic andesite magma with 54–56 wt.% SiO_2 (Alvarado, 1993; Clark et al.,

1998; Alvarado et al., 2006). Common phenocrysts include olivine, Cr-spinel, clinopyroxene, orthopyroxene, plagioclase and magnetite (Alvarado, 1993). Amphibole and biotite appear late in Irazú's crystallization sequence, generally in samples with >60% SiO_2. Allègre and Condomines (1976) used ^{238}U–^{230}Th systematics to predict that magma under Irazú has been differentiating for 140,000 years. Irazú magmas record both Th-excess and Ra-excess disequilibrium (Clark et al., 1998), which is unusual for arc magmas. As noted above, Irazú magmas also share many geochemical features of ocean island basalts, such as high Nb abundances (>15 ppm), steep REE patterns (Fig. 3b), high Ce/Pb (15–20), low Ba/La (Fig. 2a), and low B/La (Alvarado, 1993; Leeman et al., 1994; Clark et al., 1998; Carr et al., 1990). These characteristics are typical of volcanism within the CAVA segment from Platanar to Turrialba, which includes Irazú.

No published measurements or estimates exist of the water content of Irazú magmas. Such measurements must be made within melt inclusions (MI), because every magma degasses most of its H_2O upon ascent, due to the dramatic decrease in the solubility of H_2O in melt at low pressure. Melt trapped within early-formed phenocrysts, such as olivine, may still contain their pre-eruptive magmatic water concentrations, if trapped at depth and rapidly quenched (e.g., Anderson, 1979; Sisson and Layne, 1993; Sobolev and Chaussidon, 1996, Hauri, 2002). Prior studies of volatiles in CAVA MI have related magmatic water to volcanic explosivity (Roggensack et al., 1997), degree of melting in the mantle (Walker et al., 2003), crystal size (Roggensack, 2001a,b), and magmatic fractionation trends (Wade et al., 2006). These studies have also found a wide range of H_2O contents in CAVA mafic MI, from <1 wt.% in back-arc volcanoes from Guatemala (Walker et al., 2003) to ~6 wt.% in Cerro Negro volcano in Nicaragua (Roggensack et al., 1997), near the peak in Ba/La (Fig. 2a). In Guatemala, where Ba/La is lower than at Cerro Negro, mafic MI also contain less water (average ~2 wt.% for Pacaya and ~4 wt.% for Fuego; Sisson and Layne, 1993; Roggensack, 2001b; Walker et al., 2003). The only published water contents for a Costa Rican volcano are from Arenal volcano (Wade et al., 2006), which contains up to 4 wt.% water and intermediate Ba/La (~40). This study was initiated to provide the first measurements of magmatic water contents near the Ba/La minimum, at Irazú.

Because we are largely interested in the ultimate source of Irazú magmas, our goal is to measure H_2O and other volatiles in the most mafic melts trapped in the most forsteritic olivine phenocrysts. We restrict our sampling to the smallest diameter tephra possible (Luhr, 2001), as MI in lava samples typically require homogenization, and/or have suffered diffusive loss of H from the MI during cooling (e.g., Hauri et al., 2002) or major element exchange (Gaetani and Watson, 2002).

Samples from the 1723 and 1963–1965 eruptions of Irazú Volcano were collected in January, 2003, from the southwest corner of the Main Crater (Table 1). Scoria samples from the 1963–1965 eruption were collected at the top of the crater, and consist of individual bombs ranging in size from 7 to 10 cm from a single tephra layer.

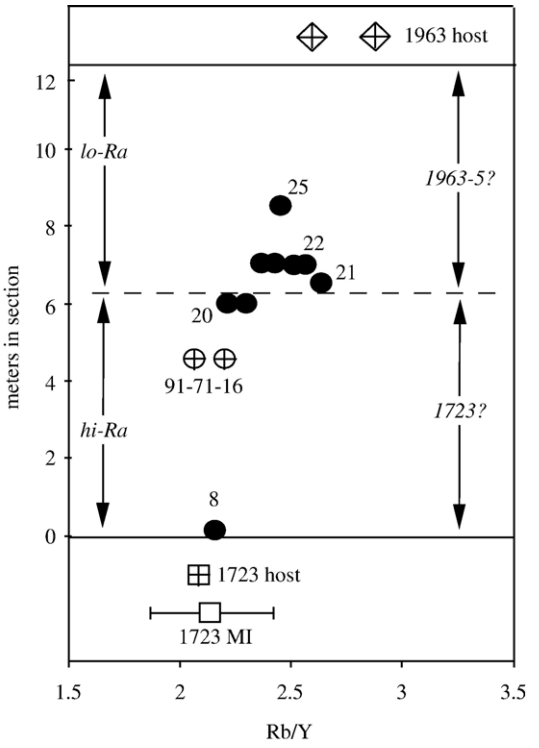

Fig. 4. Relationship between samples studied here (open symbols), and those studied by Clark et al. (1998) (within stratigraphic section, and noted by sample number). Clark et al. (1998) interpreted all of their samples as deriving from the 1963–65 eruption but noting a change within their section in the (^{226}Ra)/(^{230}Th) activity ratios, which correlate with subtle but systematic shifts in a number of trace element ratios (see their Figure 3). The shift is illustrated here with Rb/Y, where high-Ra samples have Rb/Y<2.3 and low-Ra samples have Rb/Y>2.3. The high-Ra samples are geochemically similar to our 1723 sample, and the low-Ra samples are similar to our 1963 sample, and this similarity extends to a large number of major and trace elements (e.g., MgO–FeO, Ba/Th, Li/Yb, Cs/La). Thus, the section studied by Clark et al. (1998) may include tephra from both the 1723 and 1963 eruptions, with the break between high-and low-Ra samples defining the boundary. The average of the melt inclusions (MI) from the 1723 sample is the same as the host, within the larger uncertainty in the MI analyses and population (error bar is one standard deviation of the mean). For the whole rock samples, the error bars are the size of the symbols. The unusual high-Ca MI from 91-71-16 plots off the diagram at Rb/Y 1.2 (see Sections 3.2 and 3.4).

These bomb samples (IZ03-19b1, 2) yielded only degassed, evolved melt inclusions in low Mg# clinopyroxenes (see below). Scoria samples from the 1723 eruption, which are the primary focus of this study, were collected from lapilli (IZ03-17a) within a unit approximately 10 m into the crater below the safety fence. This

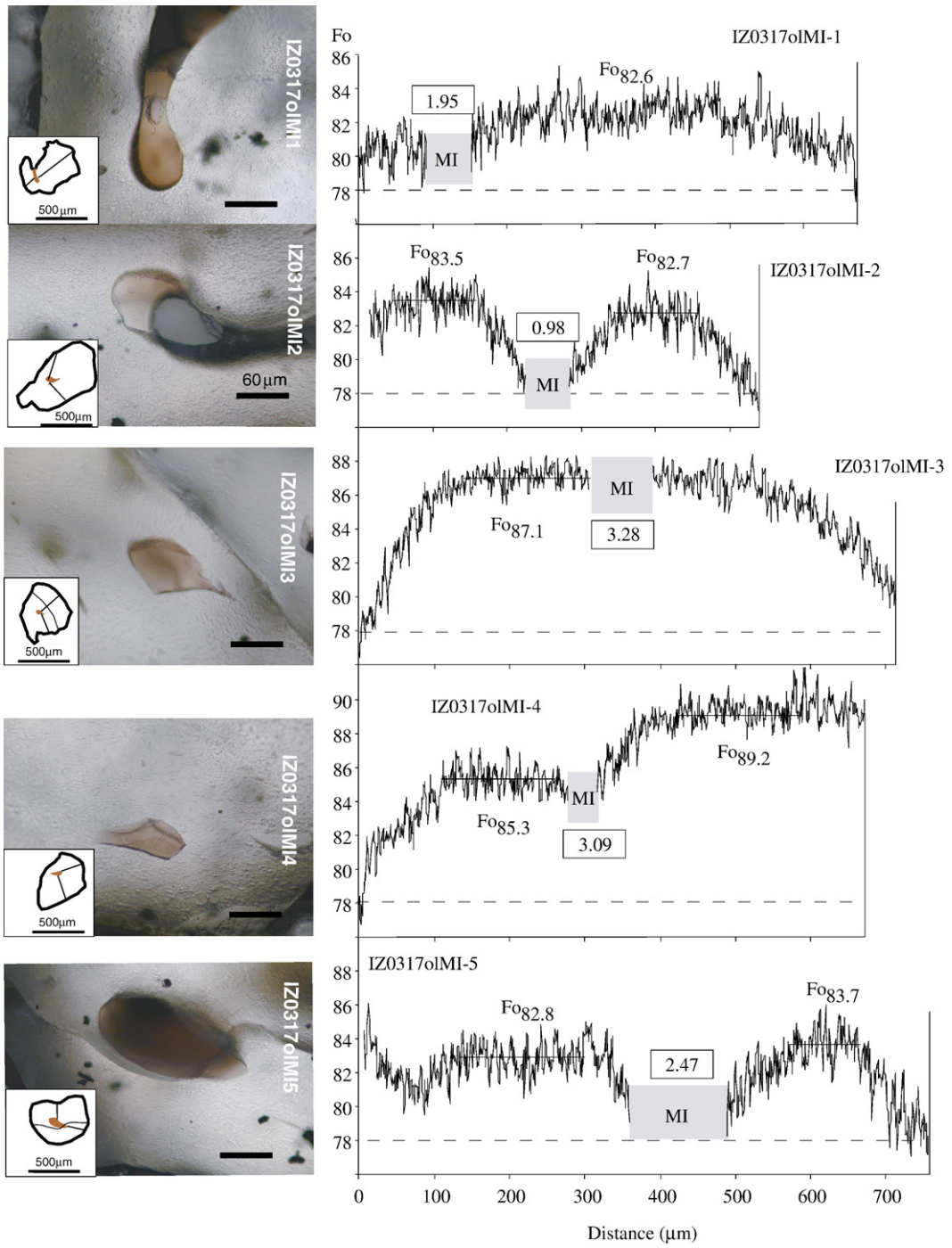

Fig. 5. Photographs (transmitted light) of olivine-hosted melt inclusions (left), and compositional profiles of olivine hosts (right). Location of melt inclusion (MI) along profile shown schematically. Average forsterite (Fo) compositions shown for olivine cores. Water contents measured in melt inclusions given in wt.% in boxes (Table 2). All graphs, photos and sketches at a common scale. Forsterite measured by laser-ablation-ICPMS in raster mode, using10 Hz repeat rate, beam expander 100%, iris 10%, power 50% (0.2 mJ/pulse), resulting in ablated trench ~20 µm in width (shown as lines in olivine sketches).

Table 2
Major element and volatile concentrations in Irazu melt inclusions

Sample	IZ03-17a	IZ03-17a	IZ03-17a	IZ03-17a	IZ03-17a	IZ03-17a	IZ03-17a	91-71-16
Inclusion	ol-MI-1	ol-MI-2	ol-MI-3	ol-MI-4	ol-MI-5	ol-MI-5	ol-MI-6	ol-MI-1
Eruption	1723	1723	1723	1723	1723	1723	1723	1723
MI size (μm)	202×60	52×78	75×58	36×40	176×82	replicate[c]	140×50	225×210
MI shape	hour glass	hour glass	cuspate	cuspate	oval		oval	neg. xl
Vapor bubble (μm)	30×10	no	no	no	no		no	75×75
Host	ol-1	ol-2	ol-3	ol-4	ol-5		ol-6	ol-1
Host (near MI)	Fo80	Fo79.5	Fo87	Fo85	Fo80.5		Fo78.5	Fo87.2
Host (core)	Fo83	Fo83.5	Fo87.1	Fo89.2	Fo83.7		Fo86.4	Fo87.2
Host size (μm)	744×611	1001×679	730×722	783×532	701×566		640x590	900x750
SiO_2 (wt.%)	52.73	56.82	48.41	52.90	55.99		53.84	47.23
TiO_2	1.24	1.16	1.12	1.24	1.12		1.51	1.52
Al_2O_3	16.99	16.38	19.78	18.95	16.00		17.24	17.26
FeO	6.72	5.64	4.55	4.16	5.78		6.10	5.10
Fe_2O_3[g]	1.87	1.57	1.27	1.16	1.61		1.72	1.41
MnO	0.16	0.09	0.07	0.10	0.13		0.12	0.09
MgO	3.40	2.90	4.20	1.67	2.87		2.52	4.56
CaO	8.14	6.73	9.46	9.49	6.70		7.77	14.25
Na_2O	4.11	4.42	4.39	3.90	4.33		4.18	2.94
K_2O	2.51	2.84	2.07	2.27	2.72		3.11	1.47
P_2O_5	0.54	0.60	0.77	0.59	0.58		0.63	0.57
Total	98.28	99.09	96.02	96.38	97.74		98.73	96.41
CO_2 (ppm) SIMS	72	39	225	212	61	63	27	462
F (ppm) SIMS	1878	1612	2515	1940	1675	1688	1611	1447
S (ppm) SIMS	1785	878	4154	2656	1717	1704	1737	3270
S (ppm) EMP	1098	1233	4200	1350	1616		1639	2562
sulfate/total S[e]		78%	63%		63%			
log(fO_2) ΔNNO[f]		+0.9	+0.6		+0.6			
Cl (ppm) SIMS	2136	2000	3840	2409	2063	2088	1780	1750
Cl (ppm) EMP	2043	2089	2812	2517	1674		2123	1738
H_2O Diff. (wt.%)[a]	1.72	0.91	3.98	3.62	2.26		1.27	3.59
H_2O Oxy (wt.%)[b]	1.62	1.03	3.66	3.28	2.44		1.74	4.08
H_2O SIMS	1.95	0.98	3.28	3.09	2.47	2.45	1.81	3.14
Olivine added[d]	4%	3%	3%	10%	5%	5%	5%	4%
SiO_2 (wt.%)	52.19	56.3	48.17	51.63	55.25		53.1	46.95
TiO_2	1.19	1.13	1.08	1.13	1.07		1.43	1.46
Al_2O_3	16.33	15.90	19.21	17.23	15.31		16.42	16.60
FeO	7.28	6.1	4.83	5.59	6.45		6.93	5.44
Fe_2O_3	1.80	1.52	1.23	1.05	1.54		1.64	1.36
MnO	0.15	0.09	0.07	0.09	0.12		0.12	0.09
MgO	4.81	3.98	5.42	5.26	4.47		4.22	6.15
CaO	7.83	6.53	9.18	8.62	6.41		7.40	13.70
Na_2O	3.95	4.29	4.27	3.55	4.14		3.98	2.83
K_2O	2.41	2.75	2.01	2.06	2.61		2.96	1.41
P_2O_5	0.52	0.58	0.75	0.53	0.56		0.60	0.55
H_2O SIMS	1.88	0.95	3.18	2.81	2.36	2.34	1.73	3.01
CO_2 (ppm) SIMS	69	38	218	192	59	60	26	445
F (ppm) SIMS	1806	1565	2442	1763	1602	1616	1534	1391
S (ppm) SIMS	1716	853	4033	2414	1643	1631	1654	3144
Cl (ppm) EMP	1964	2028	2730	2288	1602	1602	2022	1671
Total	100.91	100.59	100.34	100.23	100.79		101.05	100.22
P (H_2O-CO_2)[h]	517	170	1434	1252	708	701	363	1562
T (ol–liq)[i]	1063	1048	1054	1061	1043		1045	1074

(continued on next page)

Table 2 (*continued*)

Sample	IZ03-19b	IZ03-19b	IZ03-19b	IZ03-19b
Inclusion	cpx-MI-1a	cpx-MI-1b	cpx-MI-2a	cpx-MI-2b
Eruption	1963–5	1963–5	1963–5	1963–5
MI size (μm)	47×29	28×26	37×40	15×25
MI shape	square	round	rectangle	round
Vapor bubble (μm)				
Host	cpx-1	cpx-1	cpx-2	cpx-2
Host (near MI)	Mg#74	Mg#74	Mg#73.8	Mg#73.8
Host (core)	Mg#74	Mg#74	Mg#73.8	Mg#73.8
Host size (μm)	1010×451	1010×451	602×1076	602×1076
SiO_2 (wt.%)	61.50	61.91	62.06	63.22
TiO_2	2.09	1.87	1.14	1.45
Al_2O_3	15.08	15.12	15.55	15.00
FeO	3.51	3.49	3.67	3.20
Fe_2O_3 [g]				
MnO	0.08	0.07	0.11	0.08
MgO	1.29	1.28	1.70	1.20
CaO	3.38	3.39	3.58	2.99
Na_2O	3.23	3.73	4.37	4.52
K_2O	4.25	4.10	4.07	4.42
P_2O_5	0.68	0.43	0.84	0.37
Total	95.13	95.44	97.12	96.47
CO_2 (ppm) SIMS	21	53	n/a	30
F (ppm) SIMS	1820	2000	1750	866
S (ppm) SIMS	139	107	204	149
S (ppm) EMP	193	0	75	0
sulfate/total S [e]				
log(fO_2) ΔNNO [f]				
Cl (ppm) SIMS	1493	1371	1301	632
Cl (ppm) EMP	0	1308	1719	1664
H_2O Diff. (wt.%) [a]	4.87	4.56	2.88	3.53
H_2O Oxy (wt.%) [b]	4.32	0.85	1.12	b.d.l.
H_2O SIMS	0.71	0.82	0.63	0.24
Olivine added [d]				
SiO_2 (wt.%)	61.50	61.91	62.06	63.22
TiO_2	2.09	1.87	1.14	1.45
Al_2O_3	15.08	15.12	15.55	15.00
FeO	3.51	3.49	3.67	3.20
Fe_2O_3	0.00	0.00	0.00	0.00
MnO	0.08	0.07	0.11	0.08
MgO	1.29	1.28	1.70	1.20
CaO	3.38	3.39	3.58	2.99
Na_2O	3.23	3.73	4.37	4.52
K_2O	4.25	4.10	4.07	4.42
P_2O_5	0.68	0.43	0.84	0.37
H_2O SIMS	0.71	0.82	0.63	0.24
CO_2 (ppm) SIMS	21	53	n/a	30
F (ppm) SIMS	1820	2000	1750	866
S (ppm) SIMS	139	107	204	149
Cl (ppm) EMP	*1493*	1308	1719	1664
Total				
P (H_2O-CO_2) [h]				
T (ol–liq) [i]				

scoria deposit was formed during the early stages of the eruption. An additional mafic MI comes from a scoria sample (91-71-16) studied in Clark et al. (1998), and classified as 1963–1965, based on a modern ^{14}C age (≤200 years) of charcoal beneath the scoria (Clark et al., 2006). Given the stratigraphic descriptions in Alvarado (1993) and Clark et al. (1998), however, it appears that both samples derive from the same scoria unit, despite the disagreement as to its absolute age. Thus, what Clark et al. (1998) define as high-Ra samples of the lower, lapilli-dominated part of the 1963–1965 section, Alvarado et al. (2006) classify as 1723 scoria, based on a unconformity manifest in several sections, as well as geochemical and mineralogical distinctions between the two eruptions (Carr and Walker, 1987; Alvarado, 1993; Alvarado et al., 2006). Given the subtle, but systematic geochemical differences between the 1723 and 1963–5 eruptives, the break between the high-Ra and low-Ra samples in Clark et al. (1998) may coincide with the boundary between the 1723 and 1963–5 eruptions (Fig. 4). For the purposes of this study, we consider the mafic MI from IZ03-17a and 91-71-16 to derive from the same eruption, which the similarity in their bulk rock composition supports (Figs. 4, 6). For convenience of discussion, and because most of our MI are classed as 1723, we will refer to our results as bearing on the 1723 eruption, while noting that Clark et al. (1998) consider sample 91-71-16 to be derived from the 1963–1965 eruption.

2. Samples and methods

2.1. Sample preparation

Samples were crushed in a hydraulic press, then sieved and hand-picked for phenocrysts bearing large (>30 μm), undevitrified, naturally glassy MI (Fig. 5). Crystals were mounted in dental resin, and polished on one side. Prior to SIMS analysis, crystals were removed from the dental resin using a soldering iron, and pressed into a 1 in. diameter disk of indium metal. Viable MI were extremely rare. In IZ03-17a, only seven olivine-hosted MI were found in more than 300 g of sample. In IZ-03-19b, rare olivines were mostly free of MI, and any present were small or devitrified, and so this sample yielded no viable olivine-hosted MI. This sample did contain abundant clinopyroxene-hosted MI, but these turned out to be evolved (SiO_2>60%) and degassed (S<200 ppm, Table 2).

2.2. Analytical methods

Major element concentrations in phenocrysts and MI (Tables 2) were measured on the Jeol Superprobe 733 electron microprobe (EMP) at the Massachusetts Institute of Technology using the methods described in Wade et al. (2006). Preliminary H_2O contents of MI were calculated from EMP data in two ways: 1) by difference from 100% of the sum of the major oxides (e.g., the sum deficit technique of Anderson, 1979; Sisson and Layne, 1993), and 2) by measurement of oxygen, and attributing oxygen in excess of major oxides to water (Gaetani and Grove, 1998). The shift in the sulfur K-alpha peak was measured at the American Museum of Natural History in New York, following methods described in Mandeville et al. (2007).

Volatile elements (H, C, Cl, F, S) in MI were measured on the Cameca IMS 6f ion microprobe at the Carnegie Institute of Washington, Department of Terrestrial Magnetism (Table 2). Procedures followed those in Hauri et al. (2002) and Hauri (2002), and included a primary beam (5–10 nA) accelerated to 10 kV to create a 20–40 μm spot size. One large MI (>100 μm; IZ0317olMI5; Fig. 5, Table 2) permitted two SIMS spot measurements, which indicate excellent precision (agreement within 1% relative for H_2O, Cl, F, and S, and 2% relative at 60 ppm CO_2). SIMS H_2O measurements show excellent agreement with estimates derived from the EMP data, both by the sum deficit and excess oxygen technique (generally within 0.4 wt.% H_2O on average between the techniques). We assume most of this uncertainty lies within the EMP estimates, and so in the following discussion, we refer to the SIMS data.

Notes to Table 2:

[a] H_2O determined by sum deficit of electron microprobe analysis.

[b] H_2O determined by electron probe excess oxygen method (Gaetani and Grove, 1998).

[c] SIMS analysis of a different spot in the same melt inclusions.

[d] Equilibrium olivine added in 1% increments until in equilibrium with adjacent host; assuming K_D=0.3 for Fe/Mg ol–liq exchange.

[e] From sulfur K-alpha shift measured on electron microprobe.

[f] log fO_2 calculated from S K-alpha and model in Wallace and Carmichael (1994); NNO calculated at 1100 °C and 3 kb from Huebner and Sato (1970).

[g] Calculated assuming 20% total Fe as Fe^{3+}(based on fO_2 from S K-alpha and Fe speciation model in pMELTS, Ghiorso et al., 2002).

[h] Pressue (bars) calculated from H_2O and CO_2, using VolatileCalc (Newman and Lowenstern, 2002), for 49% SiO_2 or actual if less, and 1050 °C.

[i] T calculated from Sisson and Grove (1993) olivine thermometer, using P, H_2O, Fe_2O_3 as given here.

Table 3
Laser ablation ICPMS analyses of olivine-hosted melt inclusions

ppm	*Isotope*[b]	IZ03-17a ol-MI-1	IZ03-17a ol-MI-2	IZ03-17a ol-MI-3	IZ03-17a ol-MI-4	IZ03-17a ol-MI-5	IZ03-17a ol-MI-6	91-71-16 ol-MI-1	BHVO-2G[a] *n*=4% RSD		BHVO-2G Kelley-03% diff	
		1723	1723	1723	1723	1723	1723	1723?				
CaO%		8.14	6.73	9.46	9.49	6.70	7.77	14.25				
Sc	45	30.6	24.8	21.8	27.5	21.4	22.4	46.4	32.0	4%	30.8	4%
TiO_2%	47	1.29	1.24	1.23	1.44	1.16	1.35	1.43	2.79	2%	2.62	7%
TiO_2%	49	1.29	1.31	1.20	1.45	1.18	1.36	1.41	2.85	5%	2.62	9%
V	51	225	182	246	248	172	242	302	303	4%	289	5%
Cu	65	237	208	152	107	166	265	109	163	3%	133	22%
Rb	85	61	73	44	56	62	78	38	11	5%	9.8	8%
Sr	88	814	650	1267	892	650	749	1015	390	7%	391	0%
Y	89	34.8	26.9	28.0	31.8	26.5	29.7	30.4	24.9	11%	26.4	−6%
Zr	90	282	307	197	264	285	290	209	171	6%	184	−7%
Nb	93	27.2	29.3	25.5	27.5	28.2	32.2	22.8	19.0	7%	19.5	−3%
Ba	138	1052	887	1148	1030	815	1038	954	138	7%	129	7%
La	139	62.1	53.8	70.2	64.1	50.3	60.1	71.7	15.6	5%	14.8	5%
Ce	140	135	105	138	139	100	126	150	41.9	3%	37.3	13%
Pr	141	14.8	13.4	15.0	17.7	11.8	13.4	18.8	5.7	6%	5.4	6%
Nd	145	67.1	43.1	62.1	57.4	42.7	52.8	67.2	25.0	12%	24.3	3%
Sm	147/149	9.55	7.81	9.37	11.33	7.09	8.40	14.00	6.16	1%	6	3%
Eu	151/153	3.20	2.41	3.28	2.95	2.01	2.36	3.77	2.18	7%	1.96	11%
Gd	160	9.56	5.62	8.11	9.73	4.35	8.42	10.67	5.64	11%	6.35	−11%
Dy	163	7.62	4.65	4.32	4.55	4.26	5.70	5.67	4.62	12%	5.39	−14%
Er	166	2.57	2.15	3.48	2.20	2.31	2.95	3.09	2.49	18%	2.49	0%
Yb	172	4.56	2.49	2.06	3.58	2.74	3.19	3.34	2.69	10%	2.04	32%
Lu	175	0.44	0.69	0.67	0.52	0.64	0.51	0.46	0.34	16%	0.3	14%
Hf	178	7.82	7.21	4.33	8.14	7.29	6.42	4.77	4.23	8%	4.46	−5%
Ta	181	1.49	1.23	1.27	1.53	1.44	1.22	0.85	1.14	18%	1.2	−5%
Pb	206/208	8.32	7.90	6.96	8.32	5.42	7.47	4.48	1.94	12%	1.61	20%
Th	232	11.80	12.54	9.74	6.85	11.98	12.00	6.77	1.10	4%	1.18	−7%
U	238	4.56	3.91	3.16	3.99	3.31	4.55	2.43	0.42	29%	0.42	0%

Laser drilling conditions: 10 Hz repetition rate; BE=0, Iris=1%; 70% power=1.3 mJ/pulse; 55 μm spot diameter. ^{43}Ca used as internal standard, with CaO from Table 2. BCR-2G used as calibration standard. BHVO-2G and BCR-2G standard values from Kelley et al. (2003).

[a] USGS glass BHVO-2G analyzed as an unknown, using same calibration as for melt inclusions.

[b] Isotope monitored on ICP-MS.

Trace elements were determined in MI via laser ablation inductively coupled plasma mass spectrometer (LA-ICPMS) on the Boston University VG Elemental PQ Excel and Merchantek/VG MicroProbeII 213nm Nd-YAG laser (Table 3). Procedures followed those described in Kelley et al. (2003) except for the following modifications. Samples were analyzed in coaxial light at a 10 Hz repeat rate and beam energy of 70% (~1.30 mJ/pulse). Setting the beam expander to zero and the iris to 1% resulted in a spot size of 55 μm. Time-resolved data were collected for 120 s including 30 s of background collected while the laser was off. USGS BCR-2G was used as the calibration standard, and ^{43}Ca was used as the internal standard. Precision on MI analyses is assessed through multiple 55 μm spots on BHVO-2G, which vary within 8% relative standard deviation on average for all elements (Table 3).

Whole rock samples were prepared for ICPMS and inductively coupled plasma atomic emission spectrometry (ICPES) solution analysis via HF-HNO_3 acid digestion and $LiBO_2$ flux fusion, respectively, and followed the procedures in Kelley et al. (2003). Major and trace element data are reported in Table 1 for the 1723 and 1963 whole rock hosts of the phenocrysts and MI.

3. Results

3.1. Major element compositions and petrography

Major element data for the 1723 and 1963 scoria analyzed in this study are typical of these eruptions (Fig. 6; Table 1). Most of these compositions are classified as high Mg# andesites (as defined by Kelemen et al., 2003), although they appear to form a continuous series with high Mg# basalts (Fig. 6). The dominant phenocrysts in 1723 and 1963 scoria are plagioclase, clinopyroxene, and olivine, with lesser amounts of

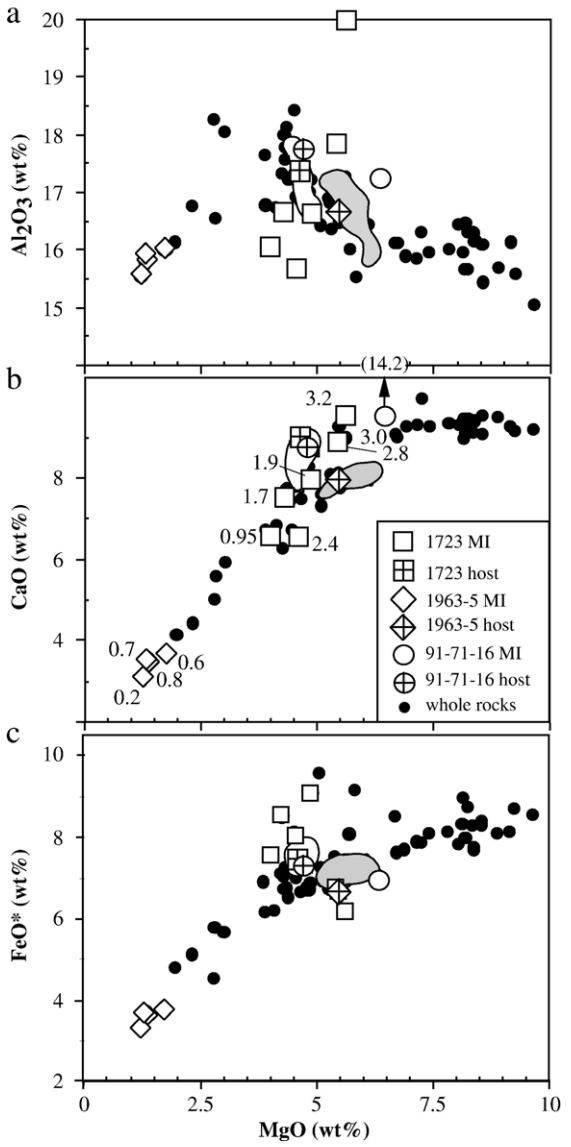

Fig. 6. Variation diagrams for Irazú volcanics (solid circles), and samples from this study (open symbols; Tables 1 and 2). Olivine-hosted melt inclusions (MI) from 1723 and 91-71-16 scoria corrected for olivine crystallization, and plotted on an anhydrous basis. MI labeled with water concentration (wt.%). All Fe reported as total FeO*. White field encloses 1723 whole rocks; dark gray field encloses 1963–1965 whole rocks from literature (Murata et al., 1966; Krushensky and Escalante, 1968; Alvarado, 1993; Clark et al., 1998; Alvarado et al., 2006; Carr et al., 2003).

orthopyroxene and oxides (see Table 1 for modes). The similar major element composition of IZ03-17a and 91-71-16 (Fig. 6) supports the correlation of these samples to the same scoria unit.

Mafic phenocrysts from the two eruptions show significant compositional variation (Fig. 7). Clinopyroxene (cpx) phenocrysts in the scoria samples range from Mg# 88 to 73. Sample IZ03-17a includes olivine compositions as primitive as Fo_{89}, while IZ03-19b includes more fractionated compositions (Fo_{70}). Fe–Mg exchange coefficients are used to estimate olivine and cpx in equilibrium with whole rock hosts and Irazú compositions as a whole (see Fig. 7 for details). The phenocrysts from IZ03-17a and IZ03-19b span the entire range expected for Irazú magmas, from primitive basalts to dacites. Nonetheless, the peaks in the olivine (Fo_{83}) and cpx (Mg#84) populations in IZ03-17a coincide with compositions estimated to be in equilibrium with the whole rock liquid. Thus, while IZ03-17a includes a large range of compositions, the majority are in equilibrium with the basaltic andesitic whole rock. In contrast, IZ03-19b includes a large population of cpx phenocrysts (and some olivines) far out of equilibrium with the whole rock host (i.e., cpx with Mg# 72–76 instead of Mg# 85; Fig. 7b). These cpx phenocrysts would have formed in an andesitic/dacitic magma similar to the melt inclusions they host (see below; Table 2), and similar to pumice inclusions in the 1723 eruptives, and older andesitic units of Irazú (e.g., Tristán and Birrís units, Alvarado et al., 2006). The 1963 scoria contains abundant evidence of mixing between felsic and mafic magmas or phenocrysts, in the coexistence of high Fo olivine (in equilibrium with basalt) and hornblende (in equilibrium with andesite), bimodal phenocryst populations, and reaction rims (Alvarado, 1993; Alvarado et al., 2006). Fewer such features are apparent in the 1723 scoria.

3.2. Melt inclusion compositions and olivine hosts from 1723 scoria

Fig. 5 shows five MI-bearing olivines from IZ03-17a. These olivines are strongly zoned, with cores ranging from Fo_{89} to Fo_{83}, and rims more uniform at ~Fo_{78}, in equilibrium with some reported brown/black matrix glass (Alvarado, 1993). MI can be found in different regions of their olivine hosts. IZ0317olMI3 (hereafter abbreviated MI3) is within a primitive (Fo_{87}) homogeneous core (Fig. 5); this is presumably a xenocryst that reacted with host magma on its rims. MI4 is associated with the most primitive xenocryst (Fo_{89}), but appears to have been trapped between two grains, one with Fo_{89} and the other with Fo_{85}. Indeed the cuspate morphology of MI4 may reflect original grain boundaries. MI2 is hourglass-shaped, and could be a selvage of liquid trapped between two nearly identical olivine grains, with $Fo_{83–84}$ cores and symmetric zoning profiles to original grain edges (one of which is now adjacent to the trapped MI2). MI5 also appears to be melt captured when two

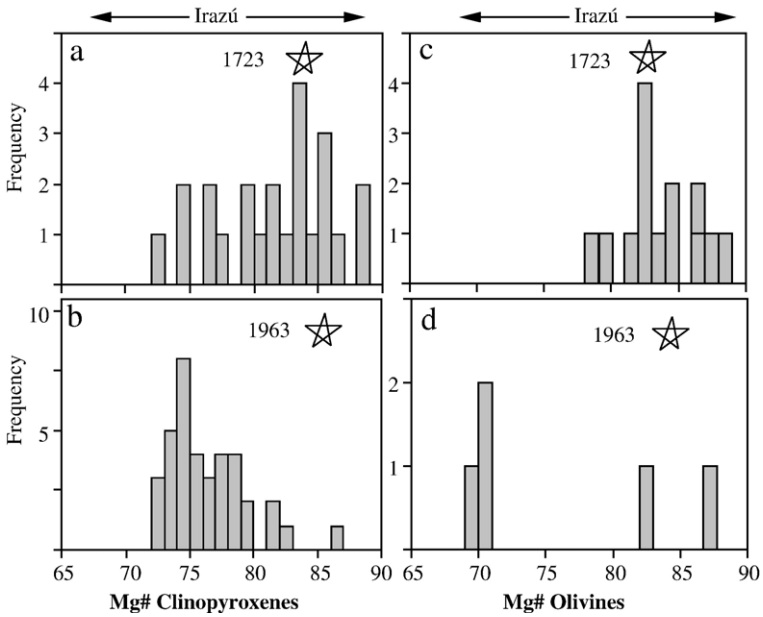

Fig. 7. Composition of Irazú clinopyroxenes (a and b) and olivines (c and d) from 1723 scoria IZ03-17a (a and c) and 1963–5 scoria IZ03-19b (b and d). Stars represent phenocryst compositions in equilibrium with whole rock compositions (Table 1), assuming K(Fe/Mg)=0.3 for olivine/liquid and 0.27 for clinopyroxene/liquid, and assuming that the whole rock compositions reflect liquids. Arrows at top of diagrams represent total range in phenocryst compositions in equilibrium with all Irazú rock compositions, using same K as above. Phenocryst microprobe data appear in Data Supplement Tables 1 and 2.

olivine grains annealed, and a crack through the grain near the melt inclusion supports this interpretation (Fig. 5). Aside from the two strongly xenocrystic olivines ($Fo_{87–89}$), there is a common core composition to the other olivines ($Fo_{83+/–0.5}$). These core compositions correspond to the population peak of IZ03-17a olivines, which are in equilibrium with the host scoria. Taken together, these olivines represent both xenocrysts ($Fo_{85–89}$) and phenocrysts (Fo_{83}), with rims (Fo_{78}) that may have equilibrated with erupted residual liquid.

All Irazú MI (now quenched glass) are in equilibrium with olivines with lower Fo than their adjacent hosts. This is commonly observed in olivine-hosted MI, and is usually ascribed to post-entrapment crystallization of olivine on the melt inclusion wall (e.g., Sisson and Layne, 1993; Cervantes and Wallace, 2003a). The amount of added olivine necessary to achieve equilibrium with the host is <5% for most of the MI (Table 2). Prior to correction, the inclusions all have <5% MgO, are more fractionated than the whole rock hosts, and scatter on variation diagrams. After correction, the MI form a tighter array, which overlaps substantially with scoria compositions. In particular, the MgO–CaO compositions of the corrected 1723 MI form an array that overlaps the Irazú whole rock array, and likely represents a liquid line of descent along an ol–plag–cpx cotectic. The average of the six MI is remarkably similar to the scoria host, within 5% relative for SiO_2, Al_2O_3, TiO_2, FeO, MgO (CaO is 10% low and the incompatible elements are 20% high). This provides further evidence that the MI record 1723 melt compositions, and have not suffered protracted diffusional re-equilibration (e.g., Gaetani and Watson, 2002). Notably, the FeO contents of the 1723 MI do not reflect the kind of Fe-loss, re-equilibration phenomenon typical of MI with long magmatic residence times (Danyushevsky et al., 2000, 2002).

Water contents in 1723 olivine-hosted MI range from 0.95 to 3.2 wt.%, and correlate with MI morphology and Fo content of the adjacent olivine. MI3 and MI4 have the highest H_2O concentrations (~3.0 wt.%), and are glassy, free of cracks and fully enclosed within primitive ($Fo_{87–89}$), xenocrystic olivine. MI1 and MI2 are both hourglass-shaped, and exhibit the lowest water contents, ~1.9 wt.% and 0.95 wt.% respectively. These low values most likely reflect trapping of liquid that is degassing as it evolves, or communicating with degassed liquid along the hourglass structure. MI5 has an intermediate water content of 2.4 wt.%, and may have lost water along the nearby crack. The 1723 Irazú MI are somewhat unusual in that they do not contain vapor/shrinkage bubbles, despite having high concentrations of volatile species. This could mean that primary vapor bubbles were larger than the MI, or that bubble nucleation

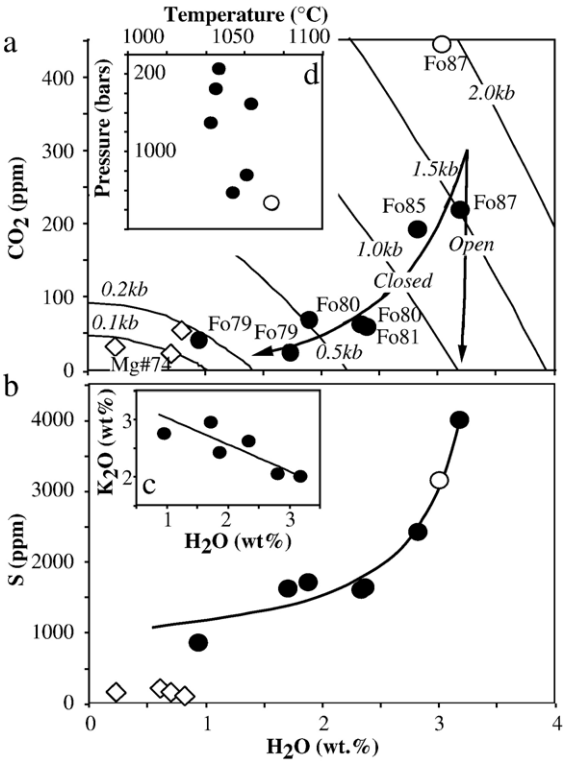

Fig. 8. a) H_2O and CO_2 concentrations in Irazú melt inclusions (Table 2), and vapor saturation isobars and degassing paths (calculated using VolatileCalc, Newman and Lowenstern, 2002). Closed circles are olivine-hosted melt inclusions from 1723 eruption, corrected for post-entrapment crystallization (Table 2); open diamonds are clinopyroxene-hosted melt inclusions; open circle is high-Ca olivine-hosted melt inclusion from sample 91-71-16. Forsterite (Fo) content of olivine and molar Mg# of clinopyroxene hosts, as indicated adjacent to melt inclusion data. Open and closed system degassing paths calculated using VolatileCalc for 49% SiO_2, 1100 °C, and 2 wt.% initial exsolved vapor (for closed system path). b) H_2O and S concentrations in Irazú melt inclusions (Table 2), and model degassing path, based on the approach in Sisson and Layne (1993). Inset (c) shows K_2O-H_2O data used to calculate the proportion of H_2O in the separating assemblage of crystals and bubbles (line shows model for 7.5 wt.% H_2O vapor and 92.5% crystals) assuming D(xl/melt)=0 for K_2O. Degassing path calculated from water mass balance and D(vapor/melt)=110 for S, assuming closed-system. d) Vapor-saturation pressure (from a) vs. temperature calculated using melt inclusions and olivine-melt thermometer in Sisson and Grove (1993). Thermometer calibration has an error of +/−8 °C.

was inhibited. Despite the different morphologies, there is a strong correlation between the concentration of water in the MI and the Fo content of the adjacent olivine (Fig. 8a), suggesting a fairly simple history of MI trapping of a crystallizing, degassing magma.

H_2O also correlates strongly with the other volatile species, including CO_2 and S (Fig. 8). Comparison of MI H_2O and CO_2 to mixed-vapor saturation isobars (Fig. 8a) suggests entrapment pressures of 1.25–1.5 kb for the MI with the highest volatile concentrations in IZ03-17a, and closed-system evolution to lower pressures (<0.2 kb) for MI with lower water contents. The maximum pressure of entrapment corresponds to a depth of 6 km (assuming a crustal density of 2.6 g/cc), which is similar to the 4–5 km depth inferred for the 1963 magma body based on displacements measured from level lines between 1949 and 1963 (Murata et al., 1966; Alvarado, 1993). Alvarado et al. (2006) also note that earthquake swarms beneath Irazú typically have hypocentral depths shallower than 7 km. Thus the 1723 MI may record the intrusion and ponding of magma at 4–7 km depth, similar to geophysical measurements of the modern magma body beneath Irazú.

Forsterite contents of host olivines decrease along the IZ03-17a MI degassing path, while the olivine–liquid temperatures drop by roughly 20 °C (1045–1065 °C; calculated from the olivine–melt thermometer in Sisson and Grove, 1993, Table 2; Fig. 8d). Such a P–T–H_2O path suggests coupled degassing and crystal fractionation as magma ascends, with crystallization driven by a decrease in pH_2O and slight cooling. Such ascent-driven crystallization is similar in concept to that outlined recently for Mt. St Helens (Blundy and Cashman, 2001), Fuego (Roggensack, 2001b), and Popocatepetl (Atlas et al., 2006), although Irazú olivine-hosted MI record slight cooling upon crystallization instead of heating, as for Mt. St. Helens syneruptive plagioclase-hosted MI (Blundy et al., 2006).

1723 MI have very high S contents, up to 4000 ppm, which also decrease systematically with Fo of the adjacent olivine and H_2O (Fig. 8), consistent with the above degassing scenario. The H_2O–S degassing trend can be modeled following the approach in Sisson and Layne (1993), yielding a high vapor/melt partition coefficient for S (D_S) of 110 (Fig. 8b), higher than that calculated for either Fuego (34, Sisson and Layne, 1993) or Arenal (70; Wade et al., 2006). Although a constant D_S is clearly an over-simplification of the complexities of sulfur degassing, the high bulk D_S for Irazú is consistent with the expected lower solubility of sulfur in melt at the lower pressures of vapor saturation of Irazú melts (≤1.5 kb; Fig. 8d) compared to melt inclusions from Arenal (<2 kb; Wade et al., 2006) and Fuego (<4 kb; Roggensack, 2001b). Such partitioning is independent of the very high initial sulfur content of Irazú melts, which is consistent with the predominance of sulfate species calculated from microprobe K-alpha scans (>63% sulfate; Table 2), the high calculated fO_2 (ΔNNO+0.6 to +0.9; Table 2), and the lack of sulfide saturation in these melts and presumably in the mantle source.

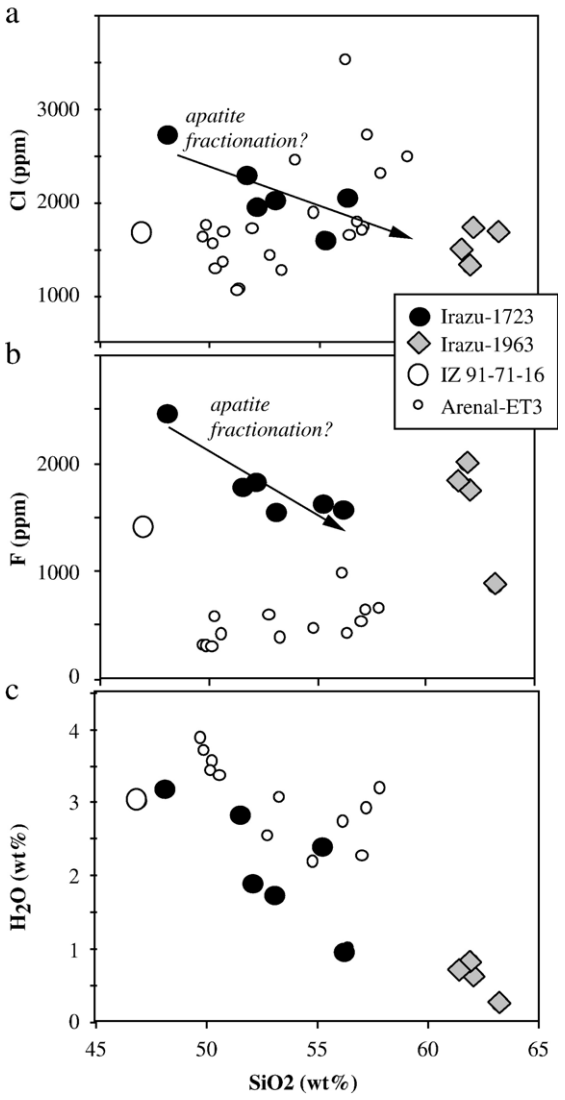

Fig. 9. Halogens and water vs. silica in Irazú and Arenal melt inclusions (from Table 2 and Wade et al., 2006). a) Cl and b) F decrease in Irazú 1723 melt inclusions as magma evolves to higher silica, which may reflect apatite saturation and fractionation in these magmas with unusually high phosphorous and fluorine contents. This is in contrast to Arenal melt inclusions, where F and Cl behave like magmaphilic incompatible elements, and phosphorous is more than a factor of three lower. c) Both volcanoes show H_2O degassing trends with increasing silica.

Cl and F also have high concentrations in 1723 MI (>2000 and >1500 ppm, respectively), and both decrease with the other volatiles as silica increases (Fig. 9). While this could reflect partitioning of halogens into the vapor, Cl and F generally have much higher solubilities in mafic melt than H_2O, S and CO_2 (e.g., Webster, 2004), and may show behavior similar to magmaphile trace elements. For example, in Arenal MI, Cl behaves much like U, indicating little loss to a vapor. On the other hand, Irazú magmas contain unusually high initial P_2O_5 concentrations, which decrease as SiO_2 increases. A kink in the SiO_2–P_2O_5 whole rock trend for the volcano led Alvarado (1993) to suggest apatite saturation in magmas with 52–53% SiO_2. This is early in the fractionation sequence for apatite, but the high F in Irazú magmas may lead to higher apatite saturation temperatures than those calculated from SiO_2 and P_2O_5 alone (which are <950 °C for the MI; Piccoli and Candela, 2002). The phosphorous systematics, along with the occurrence of apatite as an observed accessory phase in IZ03-17a and 19b (Boyce and Hervig, 2007) suggests that apatite fractionation may be the primary control on Cl and F contents in Irazú magmas.

An olivine from 91-71-16 (from the same deposit as IZ03-17a) yielded a basaltic MI with H_2O and S similar to the least degassed of the IZ03-17a MI (Fig. 8b). The Cl and F in this inclusion are somewhat lower, and CO_2 much higher than the IZ03-17a MI (Figs. 9 and 8a). The H_2O–CO_2 vapor saturation pressure (1.5 kb) is similar to the highest recorded from IZ03-17a, if calculated using the lower SiO_2 of 47 wt.% and VolatileCalc1.1 of Newman and Lowenstern (2002). This 91-71-16 MI also has a very high CaO content of >13 wt.%, which is several weight percent higher than any other Irazú composition (all of which are <10 wt.%: Fig. 6b). The high CaO, CO_2 and low SiO_2 of this MI are typical of "high-CaO" MI found sporadically worldwide (Schiano et al., 2000). Walker et al. (2003) show a link between CaO and CO_2 in Guatemalan MI, and suggest a source in subducted carbonate. If this were the case, then the Sr content of the high Ca inclusion should be higher than that of the low Ca inclusions; this is not observed (compare 91-71-16 to MI3, hosted in similar Fo_{87} olivines; Table 3). On the other hand, 91-71-16 MI has almost twice the Sc concentration of all the other MI (50 ppm Sc vs. 20–30 ppm; Table 3), consistent with dissolution of cpx (which have 70–80 ppm Sc in these samples, based on our unpublished laser ablation ICPMS data). Thus, we agree with Schiano et al. (2000) and Danyushevsky et al. (2004) that the high CaO MI derive from cpx dissolution or melting reactions in the magma storage region (≥1.5 kb or 6 km depth).

3.3. Melt inclusion compositions and olivine hosts from 1963–5 scoria

Although sample IZ03-19b yielded no viable olivine-hosted MI, it contained abundant dacitic cpx-hosted MI (Table 2). These melts are close to equilibrium with the

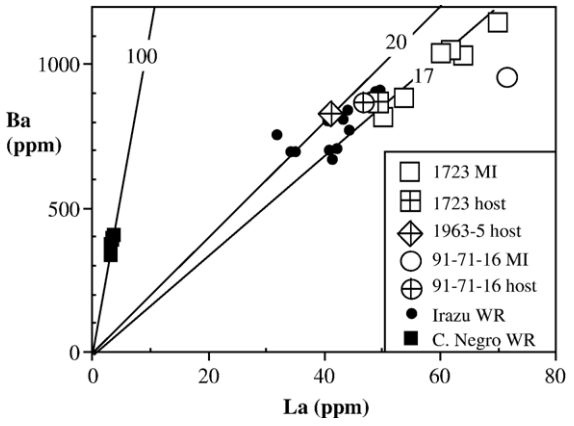

Fig. 10. Irazú melt inclusions (MI) and scoria hosts from this study, compared with other Irazú and Cerro Negro whole rocks (Carr, CentAm database, 2007). Lines are constant Ba/La.

host cpx phenocrysts, and both melt and phenocryst represent among the most evolved compositions found at Irazú (Figs. 6, 7). Such evolved magmas and phenocrysts have only erupted from Irazú twice in the past, as banded dacitic tephras within the Tristán and Birrís units (Alvarado, 1993). It is possible the evolved IZ03-19b cpx's are derived from those older units and incorporated in the more mafic 1963–5 erupting magma. The cpx-hosted MI record water contents from 0.2 to 0.8 wt.%, and have similarly low CO_2 (<55 ppm) and S (<200 ppm; Table 2). These MI record the lowest saturation pressures (<0.2 kb), and most degassed compositions (Fig. 8a), and thus equilibrated at shallow depths (<500 m).

3.4. Trace element compositions

Whole rock and MI samples from this study have trace element compositions within the range of Irazú magmas. For example, Ba/La in IZ03-17a and IZ03-19b scoria vary from 17 to 20, as do virtually all Irazú magmas (Fig. 10). The olivine-hosted MI from IZ03-17a have Ba/La nearly identical (16–17) to the 1723 host magma (17). Thus, with the exception of the unusual high Ca inclusion in 91-71-16 (which has an anomalously low Ba/La of 13, also consistent with incorporation of low Ba/La cpx), the trace element data support the notion that the 1723 MI, phenocrysts and xenocrysts are related to the host magma, and are not exotic material from the lower crust (Dungan and Davidson, 2004) or mantle (Saal et al., 1998). The constant Ba/La in the IZ03-17a MI provides additional evidence that the water variations in the MI are due primarily to degassing, and not to intrinsic variations of water in the source (which would be expected to correlate with trace element ratios; Cervantes and Wallace, 2003b).

3.5. Summary of H_2O systematics in Irazú magmas

In summary, MI from 1723 scoria provide a coherent suite of liquids that record coupled crystal fractionation and degassing during ascent and cooling (Fig. 8). The average major element composition of the MI are similar to the host scoria (Fig. 6). All volatiles (H_2O, CO_2, S, Cl and F) have suffered losses to vapor (Fig. 8) and/or apatite (Fig. 9), and thus MI measurements reflect concentration minima. Nonetheless, the shape of the H_2O–S degassing trend in particular (Fig. 8b) suggests a maximum H_2O content of ~3.5 wt.% for 1723 magmas. It is important to emphasize that the highest H_2O concentrations are recorded in basaltic MI (<52% SiO_2, Table 1), trapped in the most forsteritic olivines ($\geq Fo_{87}$), and so are not likely a product of crustal processing or sources, but derived from mantle melts. The constancy of Ba/La in the MI, and similarity with Ba/La in the whole rocks (Fig. 10), supports this view.

4. Discussion

4.1. The volatile-rich nature of Irazú magmas

The above results place minimum constraints on the volatile content of Irazú basaltic magmas. The most primitive olivines ($Fo_{85–87}$) in the 1723 scoria (including 91-71-16) contain MI with the highest water contents (2.8–3.2 wt.% H_2O), as well as the highest CO_2 (>400 ppm), S (>2500 ppm), Cl (>2000 ppm) and F (>1500 ppm). Given that the 1723 magma does not appear to be compositionally remarkable within the context of other Irazú magmas (Figs. 6, 10), these values may be typical for Irazú as a whole. Note Sadofsky et al. (2004) report higher volatile contents for a single olivine-hosted 1963 MI, up to 5 wt.% H_2O, with others in the range reported here. Nonetheless, taking the systematic results for the 1723 MI, we propose 3.2–3.5 wt.% H_2O in Irazú basaltic liquids. The lower value of this range is the maximum H_2O observed in MI3, and the upper range is a conservative maximum based on the asymptotic H_2O–S–CO_2 degassing paths in Fig. 8.

Such a water content for Irazú parental magmas (3.2–3.5 wt.%) is significantly higher than found in back-arc volcanoes in Guatemala (Fig. 11a), or common MORB or ocean island melts (Dixon et al., 2002). Published models that derive Irazú magmas from an enriched mantle source predict low water contents (~1 wt.%), as

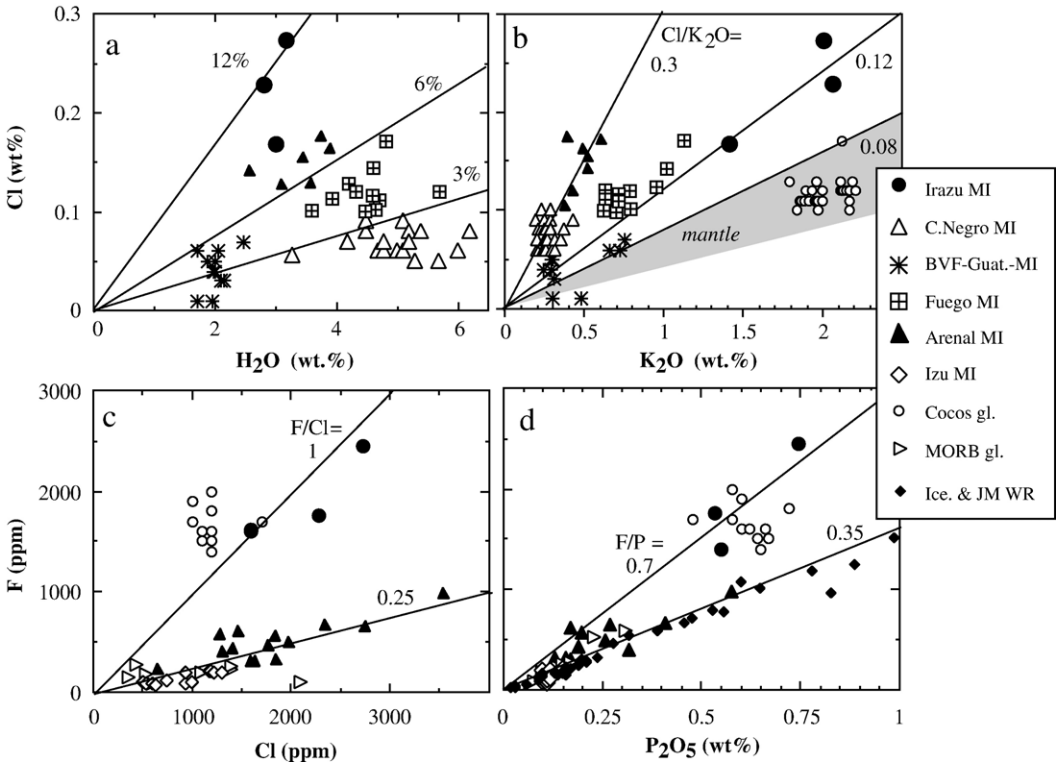

Fig. 11. Volatile species in Irazú melt inclusions (MI) compared with those in other Central American MI. a) Cl vs. H_2O, with lines of constant Cl/H_2O, and calculated wt.% salinity (after Kent et al., 2002). b) Cl vs. K_2O, with shaded "mantle" field as maximum Cl/ K_2O in MORB and OIB from Lassiter et al. (2002). Other lines are range of Cl/K_2O in Central American MI. c) F vs. Cl with lines of constant F/Cl. d) F vs. P_2O_5 with lines of constant F/P. Data in a) and b) screened to include only those least degassed in S and CO_2 (as noted below). Data sources: Irazú MI (Table 2; CO_2>150 ppm); Cerro Negro MI (Roggensack et al., 1997; Roggensack, 2001a; S>1000 and CO_2>200 ppm); Guatemala MI from behind the volcanic front (Walker et al., 2003; S>1000 and CO_2>200 ppm); Fuego MI (Sisson and Layne, 1993; Roggensack, 2001b; S>1000 ppm); Arenal MI (Wade et al., 2006; S>1000 ppm; K_2O calculated from P_2O_5*3.2 to rectify problem with alkali-loss); Izu MI (Straub and Layne, 2003;<53% SiO_2); volcanic glasses from seamount province near Cocos ridge (Hoernle et al., 2000); MORB glasses (F from Michael and Schilling, 1989; P_2O_5 from Schilling et al., 1983); Iceland and Jan Mayen volcanic rocks (non-apatite saturated, Stecher, 1998). Note different datasets on different plots due to lack of comprehensive data in other suites (e.g., no F for other Central American MI; no H_2O for Cocos glasses).

outlined in the introduction. Our results are clearly in conflict with this view. In order to derive a magma with >3.2 wt.% H_2O from enriched mantle with 0.04 wt.% H_2O, the degree of mantle melting would have to be unreasonably low, <0.055%. Thus, the water contents of Irazú magmas are not consistent with derivation from such a source. In fact, water contents at Irazú are typical of that found in many arc volcanoes, and are within the peak in the global arc MI population at 2–4 wt.% H_2O (Newman et al., 2000; Wallace, 2005). Thus, while other geochemical tracers are unusual in Irazú for an arc volcano (low Ba/La and high La/Sm), water is not.

Compared to MI from other volcanoes in the Central American volcanic arc (CAVA), Irazú basaltic MI contain lower water concentrations (3.2–3.5 wt.% vs. 4–6 wt.% for Cerro Negro, Fuego, and Arenal; Sisson and Layne, 1993; Roggensack et al., 1997; Roggensack, 2001a,b; Wade et al., 2006). However, Irazú MI are trapped in more forsteritic olivine ($Fo_{85–87}$) than those from Cerro Negro (<Fo_{82}, Roggensack, 2001a), Fuego (<Fo_{77}, Roggensack, 2001b; Sisson and Layne, 1993) or Arenal (<Fo_{79}, Wade et al., 2006), and if compositions are corrected for crystal fractionation by adding equilibrium olivine until melt is in equilibrium with mantle olivine (Fo_{90}), then the water content of primary Irazú melts (3.0 wt.% H_2O based on MI3) approaches that in other CAVA volcanoes (3–3.5 wt.%). Converting these water contents to fluxes requires an estimate of the magmatic flux. A recent study of the extrusive volcanic flux from Nicaragua to Costa Rica (Carr et al., 2007) finds no significant variations along-strike, within the large uncertainties in the volume and age estimates. Given this result, then both the water content and the water flux for Irazú primary magmas are comparable to those for other volcanoes along the CAVA. This is unexpected considering the many other geochemical

indicators that have suggested minimal slab contributions at Irazú.

The sulfur, chorine and fluorine concentrations in the least degassed Irazú MI dwarf those in most other CAVA MI, even without consideration of crystal fractionation or magma fluxes. Irazú sulfur concentrations approach some of the highest values yet measured in arc MI (4000–6000 ppm S; Wallace, 2005). Even more noteworthy are the very high halogen concentrations of Irazú MI. Cl concentrations in Irazú MI are almost a factor of 2 higher than that in any other water-rich MI from CAVA (Fig. 11a). The high Cl in Irazú MI is consistent with their high K_2O, such that Cl/K_2O of Irazú falls within the range of other MI from the CAVA ($Cl/K_2O = 0.1–0.3$; Fig. 11b). The F contents of Irazú MI are a factor of 5–10 higher than those from Arenal (Fig. 9b) and about an order of magnitude higher than those reported by Straub and Layne (2003) for the Izu arc, thus potentially increasing their global recycling flux estimates ($0.3–0.4 \times 10^{12}$ g/yr) by an order of magnitude. The high F in Irazú magma is consistent with their high P_2O_5 contents (Stecher, 1998) and Nd contents (Workman et al., 2006), given the geochemical affinity of these elements (Schilling et al., 1980), although F/P and F/Nd (not shown) is higher in Irazú than MORB or OIB (Fig. 11d).

4.2. The origin of Irazú magmas

The volatile contents of Irazú magmas provide some fresh constraints on their origin. As outlined in the Introduction, Irazú volcano is unusual in its location, volume, and composition, and most ideas concerning the origin of these features point to an unusually enriched subarc mantle, with a very low subduction signal. The conclusions above about the volatile-rich nature of Irazú argue against this origin. The high water contents (>3 wt.%) and Cl contents (>2000 ppm) for Irazú are not typical of magmas known to be derived from enriched mantle, such as ocean island basalts (generally <1.5 wt.% H_2O, Dixon et al., 1997, 2002; Workman et al., 2006; and <1000 ppm Cl; Lassiter et al., 2002). Concentrations, however, can be affected by other processes, such as the extent of partial melting in the mantle, and so elemental ratios are more diagnostic indicators of source composition. A key ratio in this regard is Cl/K_2O. If Irazú magmas were derived from OIB-type mantle, then they should have low Cl/K_2O, <0.08 (i.e., the maximum observed in MORB and OIB; Lassiter et al., 2002). For example, the Galapagos-derived Cocos plate seamount glasses have low Cl/K_2O (averaging 0.06; Fig. 11b), and so too should Irazú if it were derived from a similar mantle source. On the contrary, Irazú MI have $Cl/K_2O \geq 0.1$, well above any OIB or MORB, yet similar to that in other CAVA magmas, such as in mafic inclusions from Fuego volcano ($Cl/K_2O = 0.12–0.2$) (Fig. 11b). Cl enrichment over K in arc basalts may derive from a Cl-rich fluid from the subducting plate (Lassiter et al., 2002), and such an enrichment is additional evidence for a clear subduction signal in Irazú. This is not a subtle signal, as Irazú is more enriched in Cl and K than any other CAVA magma.

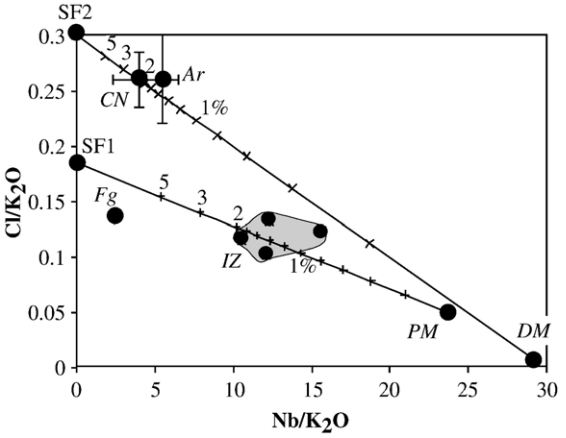

Fig. 12. Mixing between mantle (depleted mantle, DM, and primitive mantle, PM) and slab fluids (SF1 and 2) to create the source of Irazú (IZ), Cerro Negro (CN), Fuego (Fg) and Arenal (Ar) magmas. Irazú magmas could be generated by adding 1–2% of SF1 to PM, which is similar to the amount of slab fluid (SF2) needed to generate Cerro Negro and Arenal magmas from DM. In this view, Irazú is not impoverished in slab fluid components. Mixing between DM and 0.4–0.8% SF1 (not shown) could also generate Irazú magmas. DM from Salters and Stracke (2004). Nb and K_2O in PM from Sun and McDonough (1989); Cl/K_2O in PM is taken as 0.05, the maximum observed in ocean island melts compiled in Lassiter et al. (2002). Slab fluid compositions have zero Nb, and 2 wt.% K_2O (consistent with low $\delta^{18}O$ fluid in Eiler et al., 2005, and near-solidus melt at 2 GPa in Johnson and Plank, 1999). Cl in slab fluids varies to satisfy Cl/K_2O of mixing end-members for Central American magmas. Irazú data are four most primitive melt inclusions (Tables 2, 3). Fuego Cl/K_2O is average of melt inclusions in Sisson and Layne (1993); Nb/K_2O is average of whole rocks in Plank (2005). Cerro Negro Cl/K_2O is average of melt inclusions in Roggensack (2001a); Nb/K_2O is average of whole rocks in Thomas et al. (2002). Arenal average of melt inclusions in Wade et al. (2006), with K_2O recalculated as in Fig. 10.

In fact, the Cl, K and Nb systematics in Irazú MI are inconsistent with derivation from enriched mantle with a minor subduction component, as concluded in previous studies. For example, Leeman et al. (1994) calculate from B/La-$^{143}Nd/^{144}Nd$ an Irazú source of 70% primitive mantle, 30% depleted mantle, and 0.16% of a slab fluid. Eiler et al. (2005) use O isotopes in combination with trace elements to argue for an Irazú source of enriched mantle with 0.3% of a slab fluid. Fig. 12 shows

a similar slab fluid–mantle mixing model for Central America magmas, based on Cl/K_2O and Nb/K_2O. All CAVA mafic magmas are shifted to higher Cl/K_2O and lower Nb/K_2O than primitive (enriched) or depleted mantle, consistent with addition of a Cl-rich and Nb-poor fluid. Mixing between either primitive or depleted mantle and slab fluids with a range of Cl/K_2O can create the compositions of CAVA magmas. For example, Arenal and Cerro Negro sources may include 1–2% of a slab fluid mixed with depleted mantle. Irazú magmas have lower Cl/K_2O and higher Nb/K_2O, and while some of these features may require a different slab fluid composition, at face value, the lower Cl/K_2O of Irazú would require less fluid mixed with depleted mantle (0.4–0.8 wt.%). If Irazú taps primitive mantle, however, then even more fluid is needed to create the same shift in ratios (i.e., to counteract the higher K_2O in the primitive mantle), comparable to the 1–2% needed for Cerro Negro and Arenal from depleted mantle. Thus, if Irazú taps enriched mantle, its Cl/K_2O would require a flux of slab fluid comparable to that of some of the most fluid-rich volcanoes in the world. This means that Irazú would receive a large slab flux, and so the notion of a weak flux is false if the mantle is enriched.

The volatile systematics in Irazú magmas thus leads us to an alternate view. Irazú taps a fluid with higher Cl/K_2O than mantle (Fig. 12), but also with unusually high Cl/H_2O, a factor of 4 greater than Cerro Negro and seawater (Fig. 11a). Such a saline fluid might be expected to contain a high solute content, or constitute a melt. For example, Cl/H_2O in 2 GPa sediment melts in Johnson and Plank (1999) approaches and exceeds that

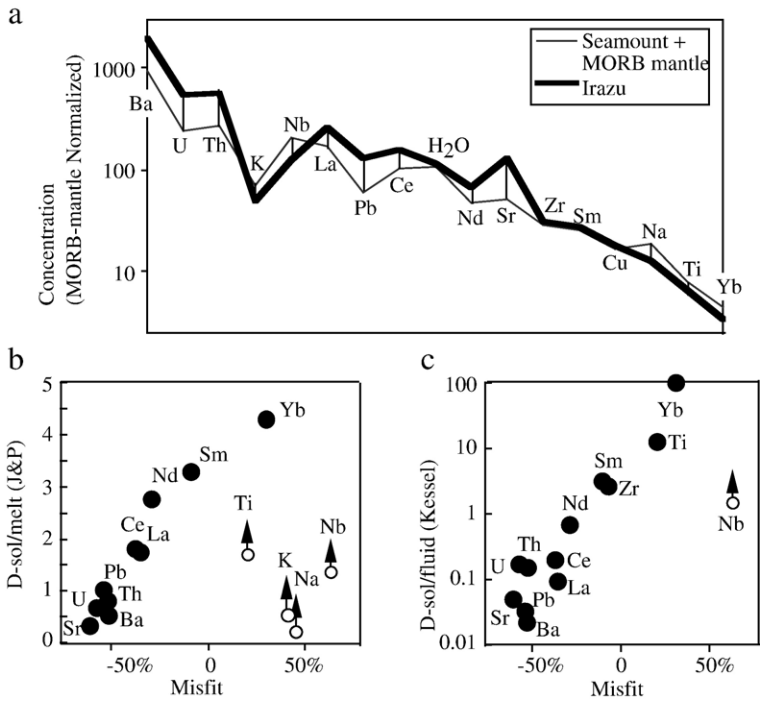

Fig. 13. Irazú source model involving mixing of subducting seamount volcanics with normal MORB mantle. a) MORB-mantle normalized concentrations for Irazú 1723 scoria host (heavy line) and mixing model results (thinner line). Figure concept and MORB mantle values from Eiler et al. (2005). Irazú 1723 scoria (Table 1) concentrations reduced by a factor of 1.4 to correct for crystal fractionation to primary concentrations (factor of 1.1 used for more compatible elements, Sr, Na and Ti). This correction has little effect on the over-all shape of the pattern. Seamount composition is average of samples from northern seamount province from Hoernle et al. (2000). Mixing model is for 1.7% seamount volcanics and 98.3% MORB mantle, which generates the correct $^{143}Nd/^{144}Nd$ for Irazú (0.51264; Feigenson et al., 2004) from mantle (0.51315, Eiler et al., 2005) and seamount volcanics (0.51284; Hoernle et al., 2000). Mixture was then melted 3% using mantle melting partition coefficients in Eiler et al. (2005). H_2O in seamount volcanics of 6.3 wt.% generates the correct H_2O in Irazú magma (3 wt.%). Misfit (difference between mixing model and Irazú data) is compared to experimentally determined partition coefficients (D's) from b) Johnson and Plank (1999) for sediment melting at 900 °C and 2 GPa and c) Kessel et al. (2005) for basaltic eclogite-subsolidus fluid with rutile at 900 °C and 4 GPa. There is a positive correlation between misfit and both sets of D. Open symbols with arrows are elements for which D's would have to be raised to better fit the Irazú model. This includes Ti and Nb, which are sensitive to the presence of rutile in the residual slab and its D for Nb; rutile was absent in the Johnson and Plank sediment but is implicated here in the slab beneath Irazú. Likewise, the low D's for Na and K in the Johnson and Plank experiments likely reflect the separate brine phase exsolved from this unusually Cl-rich starting composition.

of Irazú MI, consistent with the high Cl solubility of melts of intermediate composition (Webster, 2004). This unusual fluid or melt may be the cause of Irazú's unusual chemical characteristics, instead of an enriched mantle.

Why then do so many aspects of Irazú look like OIB, such as the REE pattern, and low Ba/La? One clear option, supported by seafloor geology, involves subduction of the seamount province on the Cocos plate seaward of the trench from Irazú (Fig. 1). The collection of cones, volcaniclastic aprons and extra thickness of igneous crust (von Huene et al., 2000) constitutes a large additional mass and chemical flux to the subduction zone. Such material, as altered Galapagos-OIB, would contribute a significant flux of H_2O and Cl (derived primarily from seafloor alteration of the volcanic material) and K, Ba, REE (derived primarily from the volcanics, which have very high igneous abundances of these elements). In fact, this material is more enriched in many trace elements than the pelagic sediments that subduct elsewhere along the Central American trench. Adding seamount volcanics of equal mass to pelagic sediments increases Ce by a factor of 5 (using 90 ppm Ce in average northwest seamount volcanics from Hoernle et al., 2000; and 10 ppm Ce in pelagic sediments from Plank and Langmuir, 1998), and could explain the lower H_2O/Ce in Irazú MI (200–250; Tables 2, 3) vs. that in Arenal MI (1000–2000; Wade et al., 2006) as largely a Ce effect alone, since primary H_2O is similar. This Galapagos-derived material would also lower Ba/La (Fig. 2a), and contribute an enriched Pb isotope signature to this sector of the arc (Fig. 2b).

Many of these geochemical features can also be met by eroding Cretaceous to early Tertiary Galapagos ophiolitic material from the fore-arc (Goss and Kay, 2006), but the high H_2O and Cl in Irazú magmas requires addition of these elements to the Galapagos volcanics. Actual measurement of H_2O and Cl in the seafloor vs. ophiolitic volcanic material would provide a test of the role of these different subducted inputs in the source of Irazú magmas.

While we can't exclude the presence of enriched mantle beneath Irazú, it may not be necessary. The simplest model would hold mantle composition constant along the Central American arc, and create enrichments in southern Costa Rica with the observed subducted input of Galapagos-derived material. Fig. 13 demonstrates how the Irazú trace element pattern may be reproduced with such a forward model. The simple bulk addition of volcanics from the northern seamount province (from Hoernle et al., 2002) with MORB-like mantle (Eiler et al., 2005) creates a trace element pattern that is similar in shape to the Irazú pattern (Fig. 13). The absolute abundances of elements are sensitive to the degree of crystal fractionation and mantle melting that creates Irazú tephra, but such parameters have a lesser effect on the shape of the pattern. Assuming 40% crystal fractionation and 3% mantle melting, simple bulk mixing of depleted mantle and seafloor volcaniclastics can reproduce Irazú abundances to within 50% for a wide range of trace elements (Fig. 13). Taken further, the

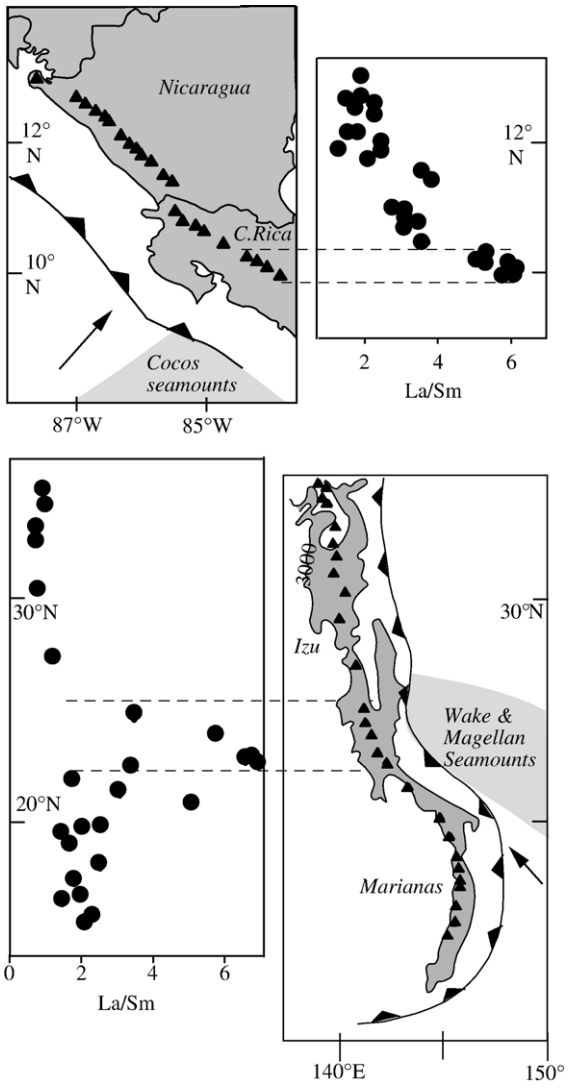

Fig. 14. Comparison of along-strike geochemical trends in Central America (top) and Izu–Bonin–Marianas (bottom). In both regions, geochemical compositions that are globally anomalous (i.e., high La/Sm; Fig. 3) correlate spatially with the subduction of ocean island type seamount chains (shown with dashed lines). Central American volcanic data from Carr (Centam database, 2007); IBM data from Peate and Pearce (1998); Elliott (2003) and Taylor and Nesbitt (1998).

elements that are most poorly fit by bulk mixing are those that are expected to be either highly incompatible in slab mineral phases (Sr, U, Ba) and so correspondingly enriched in slab liquids, or highly compatible in slab minerals (e.g., Yb in garnet) and so depleted in slab liquids. In fact, the misfit for different elements in the bulk mixing model correlates strongly with the measured partition coefficients at 900 °C, for sediment eclogite melts (Johnson and Plank, 1999) and fluids equilibrated with mafic eclogite (Kessel et al., 2005). The correlations are weaker for the 700 °C fluids of Johnson and Plank (1999) and Kessel et al. (2005), and the 650 °C pelite-fluid of Spandler et al. (2007), thus implicating higher temperature, solute-rich fluids or melts (Hermann et al., 2006) from the slab beneath Irazú. The large positive misfit (over-prediction) of the model for Nb and Ti require rutile as a residual slab phase (Schmidt et al., 2004).

Irazú trace element patterns thus resemble Galapagos OIB (Fig. 3b), but the ways in which they deviate are consistent with the predictable ways in which high temperature slab fluids may fractionate elements. Such a relationship provides powerful support for both the presence of Galapagos volcaniclastics in Irazú sources, and the experimentally-derived slab partition coefficients for different trace elements (albeit with large differences still in their absolute magnitudes; Fig. 13). This exercise demonstrates the feasibility of such a forward model to explain Irazú magmas. It differs from the inverse model developed by Eiler et al. (2005), which fits Irazú well with enriched mantle and a small slab melt component, but both the mantle and slab melt were derived in some degree from the compositions of Irazú and nearby volcanics themselves. Here we show in an independent calculation that Irazú magmas can be derived from depleted mantle and the observed volcanic material seaward of the trench.

Finally, the observations presented here for Irazú magmas may have parallels in other regions where ocean island type seamounts subduct into the mantle (Fig. 14). For example, the enormous enrichments in trace elements in Irazú are notably matched by those of the northern Marianas arc volcanoes (Fig. 3), where enriched mantle has also been invoked in the source of these shoshoniitic magmas (e.g., Stern et al., 1988). On the other hand, ocean island type seamounts of the Wake and Magellan groups (Koppers et al., 2003) are being subducted into the northern Marianas trench, and correspond spatially to large increases in the light rare earth elements (Fig. 14) and $^{206}Pb/^{204}Pb$ in the submarine volcanics of the northern Marianas arc (Lin et al., 1989; Peate and Pearce, 1998; Ishizuka et al., 2007). Once again, the high concentrations of H_2O and Cl in olivine and clinopyroxene-hosted melt inclusions from the Northern Marianas arc (1.5–3.3 wt.% H_2O and >1500 ppm Cl; Newman et al., 2000) are unusual for OIB, but may derive from the recycling of altered (hydrated) OIB volcanics through the subduction zone. Volcaniclastic turbidite sediments in the western Pacific, derived from Cretaceous seamounts, contain 5–11 wt.% mineral-bound H_2O (Karl et al., 1992), and so is appropriately hydrated to supply the arc with H_2O. Thus, the subduction of seamount chains provides an alternative explanation for geochemical anomalies along volcanic arcs, one that is more observable and testable than enriched mantle domains.

5. Conclusions

Olivine-hosted melt inclusions in 1723 tephra from Irazú volcano contain high concentrations of volatile species, notably >3 wt.% H_2O and >2000 ppm Cl. Such concentrations are atypical of magmas from ocean island sources, which have been previously implicated at Irazú. Instead, Irazú magmas are typical in their water content of arc magmas, and presumably require significant subduction and recycling of water from hydrous sources in the subducting slab. If this water and Cl are linked to altered Galapagos-derived volcanic material on the subducting Cocos plate, then this can explain the features of Irazú that are typical of both arc magmas (high H_2O, Cl, Cl/K_2O) and OIB (low Ba/La, high La/Sm). Such recycled material is also required of other geochemical observations that have been difficult to reconcile with OIB sources alone, such as Irazú's prominent negative Nb anomaly (Fig. 3b), high $CO_2/^3He$ and high $\delta^{13}C$ (Shaw et al., 2003), high $\delta^{15}N$ (Zimmer et al., 2004) and high Li/Y (Chan et al., 1999). Although we do not have water measurements for the other volcanoes within the same segment as Irazú (Platanar, Poas, Barba, and Turrialba), the similarities in their geochemical pathology (Fig. 2) suggests that this entire arc segment may be influenced by the seamount province subducting there, between the Fisher and Quepos ridges (von Huene et al., 2000; Carr et al., 2003).

Our results run counter to predictions from most previous models (e.g., Carr et al., 1990; Leeman et al., 1994; Herrstrom et al., 1995; Clark et al., 1998; Patino et al., 2000; Rupke et al., 2002; Eiler et al., 2005), in that Irazú is not obviously lacking in a slab flux of H_2O significantly more than Nicaragua volcanoes. The low Ba/La of Irazú magmas is not evidence for dry, decompression melting (Walker et al., 1995; Cameron et al., 2002), but instead subduction of low Ba/La material. Irazú magmas are most likely derived by some

form of water-fluxed melting as elsewhere (Thomas et al., 2002; Eiler et al., 2005). The subducting slab is dehydrating significantly at ~80 km (the depth to the slab beneath Irazú; Syracuse and Abers, 2006), and so some coupled thermal–thermodynamic models may require revision (e.g., Rupke et al., 2002; Gorman et al., 2006).

We would argue that previous studies favored other interpretations because they relied on elements that may not be useful proxies for water. ^{10}Be is restricted to the upper 100 m in the sedimentary section (Morris et al., 2002), whereas water will be distributed throughout the entire sedimentary column, oceanic crust, and mantle below (Rupke et al., 2002). Ba can be strongly enriched in marine sediments, and Ba/La varies worldwide by almost two orders of magnitude, unlike sediment H_2O, which varies by only a factor of 2–3 (Plank and Langmuir, 1998). Thus Ba/La variations can be driven by different inputs, independent of H_2O. Different fluids, melts and liquids from the slab may possess different U–Th fractionation (Johnson and Plank, 1999; Kessel et al., 2005), and so U-disequilibrium (Reagan, et al., 1994) may vary depending on the proportion of such phases, all of which will be hydrous. Fluids with high $\delta^{18}O$ (+25‰) and low $\delta^{18}O$ (0‰) may mix to create mantle-like $\delta^{18}O$ (+5‰; Eiler et al., 2005), with all mixtures containing significant H_2O. B may be strongly partitioned into low-T hydrous fluids, and may be a useful proxy of an isotherm (Leeman et al., 1994), but water has many hosts in the slab, some quite refractory (Poli and Schmidt, 2002). There may indeed be no substitute for direct H_2O measurements in determining the role of slab fluids in arc magma genesis.

Acknowledgements

We are grateful to Gerardo Soto for his guidance in the field; Charlie Mandeville, Mindy Zimmer, Neel Chatterjee and Louise Bolge for their assistance with analytical work; Paul Wallace and Glenn Gaetani for their discussions; and Tim Elliott for a figure. Mark Reagan graciously provided samples, and a valuable perspective on Irazú. Support for this work comes from the NSF MARGINS program (OCE-0001897 and OCE-0549051) and the NSF Instrumentation and Facilities Program (EAR-0233712).

Appendix A. Supplementary data

Supplementary data associated with this article can be found, in the online version, at doi:10.1016/j.jvolgeores.2007.08.008.

References

Abers, G.A., Plank, T., Hacker, B.R., 2003. The wet Nicaraguan slab. Geophysical Research Letters 30 (2). doi:10.1029/2002GL015649.

Allègre, C.J., Condomines, M., 1976. Fine chronology of volcanic processes using 238U-230Th systematics. Earth and Planetary Science Letters 28, 395–406.

Alvarado, G.E., Carr, M.J., Turrin, B.D., Swisher, C.C., Schmincke, H.-U., Hudnut, K.W., 2006. Recent volcanic history of Irazú volcano, Costa Rica: alternation and mixing of two magma batches, and pervasive mixing. Geological Society of America Special Paper 412, 259–276.

Alvarado, G.E., Schmincke, H.-U., 1994. Stratigraphic and sedimentological aspects of the rain-trigged lahars of the 1963–1965 Irazú eruption, Costa Rica. Zentralblatt für Geologie und Paläontologie I (1/2), 513–530.

Alvarado, G.E., 1993. Volcanology and Petrology of Irazű Volcano, Costa Rica. [Ph.D. thesis] Kiel, Christian-Albrechts-Universität zu Kiel, 261 p.

Anderson, A.T., 1979. Water in some hypersthenic magmas. Journal of Geology 87, 509–531.

Atlas, Z.D., Dixon, J.E., Sen, G., Finny, M., Martin-del Pozzo, A.-L., 2006. Melt inclusions from Volca´n Popocate´petl and Volca´n de Colima, Mexico: melt evolution due to vapor-saturated crystallization during ascent. Journal of Volcanology and Geothermal Research 153 (3–4), 221–240.

Blundy, J., Cashman, K., Humphreys, M., 2006. Magma heating by decompression-driven crystallization beneath andesite volcanoes. Nature 443, 76–80.

Blundy, J., Cashman, K., 2001. Ascent-driven crystallization of dacite magmas at Mount St. Helens. 1980–1986. Contributions to Mineralogy and Petrology 140, 631–650.

Boyce, J., Hervig, R., 2007. Apatite Volatile Barometry at Volcan Irazu, Costa Rica. AGU Fall meeting abstract.

Cameron, B.I., Walker, J.A., Carr, M.J., Patino, L.C., Matias, O., Feigenson, M.D., 2002. Flux versus decompression melting at stratovolcanoes in southeastern Guatemala. Journal of Volcanology and Geothermal Research 119, 21–50.

Carr, M.J., 2007. CentAm Database: A Geochemical Database of Volcanic Rocks from Central America. http://www-rci.rutgers.edu/~carr/index.html.

Carr, M.J., Walker, J.A., 1987. Intra-eruption changes composition of some mafic to intermediate tephras in Central America. Journal of Volcanology and Geothermal Research 33, 147–159. doi:10.1016/0377-0273(87)90058-8.

Carr, M.J., Feigenson, M.D., Bennett, E.A., 1990. Incompatible element and isotopic evidence for tectonic control of source mixing and melt extraction along the Central American arc. Contributions to Mineralogy and Petrology 105, 369–380.

Carr, M.J., Feigenson, M.D., Patino, L.C., Walker, J.A., 2003. Volcanism and geochemistry in Central America: progress and problems. In: Eiler, J. (Ed.), Inside the Subduction Factory. Geophysical Monograph, vol. 138. The American Geophysical Union, pp. 153–179.

Carr, M.J., Saginor, I., Alvarado, G.E., Bolge, L.L., Lindsay, F.N., Milidakis, K., Turrin, B., Feigenson, M.D., Swisher, C.C., 2007. Element fluxes from the volcanic front of Nicaragua and Costa Rica. Geochemistry, Geophysics, Geosystems 8. doi:10.1029/2006GC001396 22 pp.

Cervantes, P., Wallace, P., 2003a. Magma degassing and basaltic eruption styles: a case study of approximately 2000 year BP Xitle Volcano in central Mexico. Journal of Volcanology and Geothermal Research 120, 249–270.

Cervantes, P., Wallace, P.J., 2003b. Role of H_2O in subduction-zone magmatism: new insights from melt inclusions in high-Mg basalts from central Mexico. Geology 31 (3), 235–238.

Chan, L.H., Leeman, W.P., You, C.F., 1999. Lithium isotopic composition of Central American Volcanic Arc lavas: implications for modification of subarc mantle by slab-derived fluids. Chemical Geology 160 (4), 255–280.

Clark, S.K., Reagan, M.K., Plank, T., 1998. Trace element and U-series systematics for 1963–1965 tephras from Irazu Volcano, Costa Rica: implications for magma generation processes and transit times. Geochimica et Cosmochimica Acta 62 (15), 2689–2699.

Clark, S.K., Reagan, M.K., Trimble, D.A., 2006. Tephra deposits for the past 2600 years from Irazú volcano, Costa Rica. Geological Society of America Special Paper, vol. 412, pp. 225–234.

Cushman, B., Sinton, J., Ito, G., Dixon, J.E., 2004. Glass compositions, plume-ridge interaction, and hydrous melting along the Galapagos Spreading Center, 90.5 W to 98 W. Geochemstry, Geophysics, Geosystems 5. doi:10.1029/2004GC000709.

Danyushevsky, L.V., Della-Pasqua, F.N., Sokolov, S., 2000. Re-equilibration of melt inclusions trapped in magnesian olivine phenocrysts from subduction-related magmas: petrologic implications. Contributions of Mineralogy and Petrology 138, 68–83.

Danyuchevsky, L.V., Sokolov, S., Falloon, T.J., 2002. Melt inclusions in olivine phenocrysts: using diffusive re-equilibration to determine the cooling history of a crystal, with implications for the origin of olivine–phyric volcanic rocks. Journal of Petrology 43, 1631–1671.

Danyuchevsky, L.V., Leslie, R.A., Crawford, A.J., Durance, P., 2004. Melt inclusions in primitive olivine phenocrysts: the role of localized reaction processes in the origin of anomalous compositions. Journal of Petrology 45 (12), 2531–2553.

DeMets, C., 2001. A new estimate for present-day Cocos–Caribbean plate motion: implications for slip along the Central American volcanic arc. Geophysical Research Letters 28, 4043–4046.

Dixon, J.E., Clague, D.A., Wallace, P., Poreda, R., 1997. Volatiles in alkalic basalts from the North Arch volcanic field, Hawaii: extensive degassing of deep submarine-erupted alkalic series lavas. Journal of Petrology 38, 911–939.

Dixon, J.E., Leist, L., Langmuir, C., Schilling, J.-G., 2002. Recycled dehydratrated lithosphere observed in plume-influenced mid-ocean-ridge basalt. Nature 420, 385–389.

Dungan, M.A., Davidson, J., 2004. Partial assimilative recycling of the mafic plutonic roots of arc volcanoes: an example from the Chilean Andes. Geology 32, 773–776.

Eiler, J.M., Carr, M.J., Reagan, M., Stolper, E., 2005. Oxygen isotope constraints on the sources of Central American arc lavas. Geochemistry, Geophysics, Geosystems 6 (Q07007). doi:10.1029/2004GC000804.

Elliott, T.R., 2003. Tracers of the slab. In: Eiler, J. (Ed.), Inside the Subduction Factory. American Geophysical Union Monograph, vol. 138. American Geophysical Union, Washington, DC, pp. 23–45.

Feigenson, M.D., Carr, M.J., Maharaj, S.V., Juliano, S., Bolge, L.L., 2004. Lead isotope composition of Central American volcanoes: influence of the Galapagos plume. Geochemistry, Geophysics, Geosystems 5 (Q06001). doi:10.1029/2003GC000621.

Gaetani, G.A., Grove, T.L., 1998. The influence of water on melting of mantle peridotite. Contribution to Mineralalogy and Petrology 131, 323–346.

Gaetani, G.A., Watson, E.B., 2002. Modeling the major-element evolution of olivine hosted melt inclusions. Chemical Geology 183, 25–41.

Ghiorso, M.S., Hirschmann, M.M., Reiners, P.W., Kress 3rd, V.C., 2002. The pMELTS: a revision of MELTS for improved calculation of phase relations and major element partitioning related to partial melting of the mantle to 3 GPa. Geochemistry, Geophysics, Geosystems 3 (5). doi:10.1029/2001GC000217.

Gorman, P.J., Kerrick, D.M., Connolly, J.A.D., 2006. Modeling open system metamorphic decarbonation of subducting slabs. Geochemistry, Geophysics, Geosystems 7 (4), Q04007. doi:10.1029/2005GC001125.

Goss, A.R., Kay, S.M., 2006. Steep REE patterns and enriched Pb isotopes in southern Central American arc magmas: evidence for forearc subduction erosion? Geochemistry, Geophysics, Geosystems 7, Q05016. doi:10.1029/2005GC001163.

Hauff, F., Hoernle, K., van den Bogaard, P., Alvarado, G., Garbe-Schonberg, D., 2000. Age and geochemistry of basaltic complexes in western Costa Rica: contributions to the geotectonic evolution of Central America. Geochemistry, Geophysics, Geosystems 1 (5). doi:10.1029/1999GC000020.

Hauri, E., 2002. SIMS analysis of volatiles in silicate glasses 2. Isotopes and abundances in Hawaiian melt inclusions. Chemical Geology 183, 115–141.

Hauri, E., Wang, J., Dixon, J.E., King, P.L., Mandelvile, C., Newman, S., 2002. SIMS analysis of volatiles in silicate glasses 1. Calibration, matrix effects and comparisons with FTIR. Chemical Geology 183, 99–114.

Hauri, E.H., Gaetani, G.A., Green, T.H., 2006. Partitioning of water during melting of the Earth's upper mantle at H_2O-undersaturated conditions. Earth and Planetary Science Letters 259, 715–734.

Hermann, J., Spandler, C., Hack, A., Korsakov, A.V., 2006. Aqueous fluids and hydrous melts in high-pressure and ultra-high pressure rocks: implications for element transfer in subduction zones. Lithos 92, 399–417.

Herrstrom, E.A., Reagan, M.K., Morris, J.D., 1995. Variations in lava composition associated with flow of asthenosphere beneath southern Central America. Geology 23 (7), 617–620.

Hoernle, K., Heydolph, K., Sadofsky, S., Lissinna, B., Hauff, F., van den Bogaard, P., 2006. The origin of spatial and temporal geochemical variations in the Central American Volcanic Arc. Eos Trans. American Geophysical Union 87 (52) Fall Meet. Suppl., Abstract V52B-03.

Hoernle, K., van den Bogaard, Paul, Werner, Reinhard, Lissinna, B., Hauff, F., Alvarado, Guillermo, Garbe-Schönberg, C.-Dieter, 2002. Missing history (16–71 Ma) of the Galapagos hotspot: implications for the tectonic and biological evolution of the Americas. Geology 30, 795–798.

Hoernle, K., Werner, R., Morgan, J.P., Schönberg, D.G., Bryce, J., Mrazek, J., 2000. Existence of complex spatial zonation in the Galapagos plume for at least 14 m.y. Geology 28, 435–438.

Huebner, J.S., Sato, M., 1970. The oxygen fugacity-temperature relationships of manganese oxide and nickel oxide buffers. American Mineralogist 55, 934–952.

Ishizuka, O., Taylor, R.N., Yuasa, M., Milton, J.A., Nesbitt, R.W., Uto, K., Sakamoto, I., 2007. Processes controlling along-arc isotopic variation of the southern Izu–Bonin arc. Geochemistry, Geophysics, Geosystems 8. doi:10.1029/2006GC001475 20 pp.

Johnson, M.C., Plank, T., 1999. Dehydration and melting experiments constrain the fate of subducted sediments. Geochemistry, Geophysics, Geosystems 1.

Karl, S.M., Wandless, G.A., Karpoff, A.M., 1992. Sedimentological and geochemical characteristics of ODP Leg 129 siliceous deposits. In: Larson, R., Lancelot, Y., et al. (Eds.), Proc. Ocean Drilling Program, Scientific Results, vol. 129. Ocean Drilling Program, College Station, TX, pp. 31–80.

Kelemen, P.B., Hanghøj, K., Greene, A.R., 2003. One view of the geochemistry of subduction-related magmatic arcs, with and

emphasis on primitive andesite and lower crust, in The Crust (R.L. Rudnick, ed.), Vol. 3 Treatise on Geochemistry, edited by H.D. Holland, and K.K. Turekian, Elsevier, Oxford.

Kelley, K.A., Plank, T., Ludden, J., Staudigel, H., 2003. Composition of altered oceanic crust at ODP sites 801 and 1149. Geochemistry Geophysics Geosystems 4, 8910.

Kelley, K.A., Plank, T., Grove, T.L., Stolper, E.M., Newman, S., Hauri, E., 2006. Mantle melting as a function of water content at subduction zones I: back-arc basins. Journal of Geophysical Research 111, B09208.

Kent, A.J.R., Peate, D.W., Newman, S., Stolper, E., Pearce, J.A., 2002. Chlorine in submarine glasses from the Lau Basin: seawater contamination and constraints on the composition of slab-derived fluids. Earth and Planetary Science Letters 202, 361–377.

Kessel, R., Schmidt, M.W., Ulmer, P., Pettke, T., 2005. Trace element signature of subduction-zone fluids, melts and supercritical liquids at 120–180 km depth. Nature 437, 724–727.

Kolarsky, R.A., Mann, P., Montero, W., 1995. Island arc response to shallow subduction of the Cocos Ridge, Costa Rica. In: Mann, P. (Ed.), Geologic and Tectonic Development of the Caribbean Plate Boundary in Southern Central America: Boulder, Colorado. Geological Society of America Special Paper, vol. 295, pp. 235–262.

Koppers, A.A.P., Staudigel, H., Pringle, M., Wijbrans, J.R., 2003. Short-lived and discontinuous intra-plate volcanism in the South Pacific: hotspots or extensional volcanism? Geochemistry, Geophysics, Geosystems 4, 1089. doi:10.1029/2003GC000533.

Krushnesky, R.D., Escalante, G., 1968. Activity of Irazú and Poas volcanoes, Costa Rica, November 1964–July, 1995. Bulletin of Volcanology 31, 75–84.

Lassiter, J.C., Hauri, E.H., Nikogosian, I.K., Barsczus, H.G., 2002. Chlorine–potassium variations in melt inclusions from Raivavae and Rapa, Austral Islands: constraints on chlorine recycling in the mantle and evidence from brine-induced melting of oceanic crust. Earth and Planetary Science Letters 202, 525–540.

Leeman, W.P., Carr, M.J., Morris, J.D., 1994. Boron geochemistry of the Central American Volcanic Arc: constraints on the genesis of subduction related magmas. Geochimica et Cosmochimica Acta 58, 149–168.

Lin, P.N., Stern, R.J., Bloomer, S.H., 1989. Shoshonitic volcanism in the northern Mariana Arc: 2. Large-ion lithophile and rare earth element abundances; evidence for the source of incompatible element enrichments in intraoceanic arcs. Journal of Geophysical Research 94, 4497–4514.

Luhr, J.F., 2001. Glass inclusions and melt volatile contents at Paricutin Volcano, Mexico. Contributions to Mineralogy and Petrology 142, 261–283.

Mandeville, C.W., Webster, J.D., Tappen, C., Taylor, B.E., Timbal, A., Sasaki, A., Hauri, E., Bacon, C.R., 2007. Stable isotope and petrologic evidence for open-system degassing during the climactic and pre-climactic eruptions of Mt. Mazama, Crater Lake, Oregon. Geochimica et Cosmochimica Acta, in review.

Michael, P.J., Schilling, J.-G., 1989. Chlorine in mid-ocean ridge magmas – evidence for assimilation of seawater-influenced components. Geochimica et Cosmochimica Acta 53, 3131–3143.

Morris, J.D., Leeman, W.P., Tera, F., 1990. The subducted component in island arc lavas: constraints from Be isotopes and B–Be systematics. Nature 344, 31–35.

Morris, J., Valentine, R., Harrison, T., 2002. ^{10}Be imaging of sediment accretion and subduction along the northeast Japan and Costa Rica convergent margins. Geology 30, 59–62.

Murata, K.J., Dondoli, C., Saenez, R., 1966. The 1963–65 eruption of Irazú Volcano, Costa Rica (The period of March 1963 to October 1964). Bulletin of Volcanology 29, 765–793.

Newman, S., Lowenstern, J.B., 2002. VOLATILECALC: a silicate melt–H_2O–CO_2 solution model written in Visual Basic for Excel. Computers and Geosciences 28, 597–604.

Newman, S., Stolper, E., Stern, R., 2000. H_2O and CO_2 in magmas from the Mariana arc and back arc systems. Geochemistry, Geophysics, Geosystems 1 1999GC000027.

Patino, L.C., Carr, M.J., Feigenson, M.D., 2000. Local and regional variations in Central American arc lavas controlled by variations in subducted sediment input. Contributions to Mineralogy and Petrology 138, 265–283.

Peate, D.W., Pearce, J.A., 1998. Causes of spatial compositional variations in Mariana arc lavas: trace element evidence. The Island Arc 7, 479–495.

PetDB (Petrological Database of the Ocean Floor), 2007. http://www.petdb.org/.

Piccoli, P.M., Candela, P.A., 2002. Apatite in igneous systems. In: Kohn, M.J., Rakovan, J., Hughes, J.M. (Eds.), Phosphates: Geochemical, Geobiological, and Materials Importance. Reviews in Mineralogy and Geochemistry, vol. 48. Mineralogical Society of America.

Plank, T., 2005. Constraints from thorium/lanthanum on sediment recycling at subduction zones and the evolution of the continents. Journal of Petrology 46, 921–944.

Plank, T., Langmuir, C.H., 1998. The chemical composition of subducting sediment and its consequences for the crust and mantle. Chemical Geology 145, 325–394.

Plank, T., Balzer, V., Carr, M., 2002. Nicaraguan volcanoes record paleoceanographic changes accompanying closure of the Panama gateway. Geology 30, 1087–1090.

Poli, S., Schmidt, M.W., 2002. Petrology of subducted slabs. Annual Review on Earth and Planetary Sciences 30, 207–235.

Reagan, M.K., Gill, J.B., 1989. Coexisting calcalkaline and high-niobium basalts from Turrialba volcano, Costa Rica: Implications for residual titanates in arc magma sources. Journal of Geophysical Research 94 (B4), 4619–4633.

Reagan, M.K., Morris, J.D., Herrstrom, Eileen A., Murrell, Micheal T., 1994. Uranium series and beryllium isotope evidence for an extended history of subduction modification of the mantle below Nicaragua. Geochimica et Cosmochimica Acta 58 (19), 4199–4212.

Roggensack, K., 2001a. Sizing up crystals and their melt inclusions; a new approach to crystallization studies. Earth and Planetary Science Letters 187 (1–2), 221–237.

Roggensack, K., 2001b. Unraveling the 1974 eruption of Fuego volcano (Guatemala) with small crystals and their young melt inclusions. Geology 29, 911–914.

Roggensack, K., Hervig, R., McKnight, S., Williams, S., 1997. Explosive basaltic volcanism from Cerro Negro Volcano: Influence of volatiles on eruption style. Science 277, 1639–1642.

Rüpke, L.H., Phipps-Morgan, J., Hort, M., Connolly, J.A.D., 2002. Are the regional variations in Central American arc lavas due to differing basaltic versus peridotitic slab sources of fluids? Geology 30, 1035–1038.

Russo, R.M., Silver, P.G., 1994. Trench-parallel flow beneath the Nazca Plate from seismic anisotropy. Science 263, 1105–1111.

Saal, A.E., Hart, S.R., Shimizu, N., Hauri, E.H., Layne, G.D., 1998. Pb isotopic variability in melt inclusions from oceanic island basalts, Polynesia. Science 282, 1481–1484.

Sadofsky, S.J., Hoernle, K., van den Bogaard, P., 2004. The role of water in arc magmatism in Nicaragua and Costa Rica. Eos Trans. American Geophysical Union, Fall Meet. Suppl. 85 (47) Abstract V13A-1448.

Salters, V.J.M., Stracke, A., 2004. Composition of the depleted mantle. Geochemistry, Geophysics, Geosystems 5. doi:10.1029/2003GC000597.

Schiano, P., Eiler, J.M., Hutcheon, I.D., Stolper, E.M., 2000. Primitive CaO-rich, silica undersaturated melts in island arcs: evidence for the involvement of clinopyroxene-rich lithologies in the petrogenesis of arc magmas. Geochemistry, Geophysics, Geosystems 1 1999GC000032.

Schilling, J.-G., Bergeron, M.B., Evans, R., 1980. Halogens in the mantle beneath the North Atlantic. Royal Society of London Philosophical Transactions series A 297, 147–178.

Schilling, J.-G., Zajak, M., Evans, R., Johnson, T., White, W., Devine, J.D., Kingsley, R., 1983. Petrologic and geochemical variations along the Mid-Atlantic Ridge from 29°N to 73°N. American Journal of Science 283, 510–586.

Schmidt, M.W., Dardon, A., Chazot, G., Vannucci, R., 2004. Rutile-melt partitioning of Nb and Ta dependent on melt composition and Nb/Ta fractionation in the Earth. Earth and Planetary Science Letters 226, 415–432.

Shaw, A.M., Hilton, D.R., Fischer, T.P., Walker, J.A., Alvarado, G.E., 2003. Contrasting He–C relationships in Nicaragua and Costa Rica: insights into C cycling through subduction zones. Earth and Planetary Science Letters 214, 499–513.

Sisson, T.W., Grove, T.L., 1993. Temperatures and H_2O contents of low-MgO high-alumina basalts. Contributions to Mineralogy and Petrology 113, 167–184.

Sisson, T.W., Layne, G.D., 1993. H_2O in basalt and basaltic andesite glass inclusions from four subduction-related volcanoes. Earth and Planetary Science Letters 117, 619–635.

Sobolev, A.V., Chaussidon, M., 1996. H_2O concentrations in primary melts from supra-subduction zones and mid-ocean ridges: implications for H_2O storage and recycling in the mantle. Earth and Planetary Science Letters 137, 45–55.

Spandler, C., Mavrogenes, J., Hermann, J., 2007. Experimental constraints on element mobility from subducted sediments using high-P synthetic fluid/melt inclusion. Chemical Geology, 239, 228–249.

Stecher, O., 1998. Fluorine geochemistry in volcanic rocks series: examples from Iceland and Jan Mayen. Geochimica et Cosmochimica Acta 62, 3117–3130.

Stern, R.J., Bloomer, S.H., Lin, P.-N., Ito, E., Morris, J., 1988. Shoshonitic magmas in nascent arcs: new evidence form submarine volcanoes in the northern Marianas. Geology 16, 426–430.

Straub, S.M., Layne, G.D., 2003. The systematics of chlorine, fluorine and water in the Izu arc front volcanic rocks: implications for volatile recycling in subduction zones. Geochimica et Cosmochimica Acta 67, 4179–4203.

Sun, S., McDonough, W.F., 1989. Chemical and isotopic systematics of oceanic basalts: implications for mantle composition and processes. In: Saunders, A.D., Norrey, M.J. (Eds.), Magmatism in the Ocean Basins. Geological Society, London, Special Publications, vol. 42, pp. 313–345.

Syracuse, E., Abers, G., 2006. Global compilation of variations in slab depth beneath arc volcanoes and implications. Geochemstry, Geophysics, Geosystems 7, Q05017. doi:10.1029/2005GC001045 18 pp.

Taylor, R.N., Nesbitt, R.W., 1998. Isotopic characteristics of subduction fluids in an intra-oceanic setting, Izu–Bonin arc, Japan. Earth and Planetary Science Letters 164, 79–98.

Thomas, R.B., Hirschmann, Marc M., Cheng, Hai, Reagan, Mark K., Edwards, R. Lawrence, 2002. ($^{231}Pa/^{235}U$)–($^{230}Th/^{238}U$) of young mafic volcanic rocks from Nicaragua and Costa Rica and the influence of flux melting on U-series systematics of arc lavas. Geochimica et Cosmochimica Acta 66 (24), 4287–4309.

Vannucchi, P., Ranero, C.R., Galeotti, S., Straub, S.M., Scholl, D.W., McDougall-Ried, K., 2003. Fast rates of subduction erosion along the Costa Rica Pacific margin: implications for nonsteady rates of crustal recycling and subduction zones. Journal of Geophysical Research 108 (B11, 2511). doi:10.1029/2002JB002207.

von Huene, R., Ranero, C.R., Weinrebe, W., 2000. Quaternary convergent margin tectonics of Costa Rica, segmentation of the Cocos Plate, and Central American volcanism. Tectonics 19, 314–334.

Wade, J.A., Plank, T., Melson, W.G., Soto, G.J., Hauri, E.H., 2006. The volatile content of magmas from Arenal volcano. Journal of Volcanology and Geothermal Research 157, 94–120.

Waldron, H.H., 1967. Debris flow and erosion control problems caused by the ash eruptions of Irazú volcano, Costa Rica. US Geological Survey Bulletin 1241, I1–I37.

Walker, J.A., Carr, M.J., Patino, L.C., Johnson, C.M., Feigenson, M.D., Ward, R.L., 1995. Abrupt change in magma generation processes across the Central American arc in southeastern Guatemala: flux-dominated melting near the base of the wedge to decompression melting near the top of the wedge. Contributions to Mineralogy and Petrology 120, 378–390.

Walker, J.A., Roggensack, K., Patino, L.C., Cameron, B.I., Matais, O., 2003. The water and trace element contents of melt inclusions across an active subduction zone. Contributions to Mineralogy and Petrology 146 (1), 62–77.

Wallace, P.J., 2005. Volatiles in subduction zone magmas: concentrations and fluxes based on melt inclusion and volcanic gas data. Journal of Volcanology and Geothermal Research 140, 217–240.

Wallace, P.J., Carmichael, I.S.E., 1994. S speciation in submarine basaltic glasses as determined by measurements of SKa X-ray wavelength shifts. American Mineralogist 79, 161–167.

Webster, J.D., 2004. The exsolution of magmatic hydrosaline chloride liquids. Chemical Geology 210 (1–4), 33–48.

Werner, R., Hoernle, K., van den Bogaard, P., Ranero, C., von Huene, R., Korich, D., 1999. Drowned 14 m.y. old Galapagos archipelago of the coast of Costa Rica: implications for tectonic and evolutionary models. Geology 27, 499–502.

Workman, R.K., Hauri, E., Hart, S.R., Wang, J., Blusztajn, J., 2006. Volatile and trace elements in basaltic glasses from Samoa: implications for water distribution in the mantle. Earth and Planetary Science Letters 241, 932–951.

Zimmer, M.M., Fischer, T.P., Hilton, D.R., Alvarado, G.E., Sharp, Z.D., Walker, J.A., 2004. Nitrogen systematics and gas fluxes of subduction zones: insights from Costa Rica arc volatiles. Geochemistry, Geophysics, Geosystems 5, Q05J11. doi:10.1029/2003GC000651.